Journal of Medicinal Chemistry

Article

Improving the Selectivity of PACE4 Inhibitors through Modifications of the P1 Residue

Vahid Dianati, Pauline Navals, Frédéric Couture, Roxane Desjardins, Anthony Dame, Anna Kwiatkowska, Robert Day, and Yves L. Dory

J. Med. Chem., **Just Accepted Manuscript** • DOI: 10.1021/acs.jmedchem.8b01381 • Publication Date (Web): 01 Dec 2018

ACS Publications

is published by the American Chemical Society. 1155 Sixteenth Street N.W., Washington, DC 20036

Improving the Selectivity of PACE4 Inhibitors through Modifications of the P1 Residue

Vahid Dianati,[†] Pauline Navals,[†] Frédéric Couture,[‡] Roxane Desjardins,[‡] Anthony Dame,[‡] Anna Kwiatkowska,[‡] Robert Day[‡] and Yves L. Dory[†]*

†Institut de Pharmacologie de Sherbrooke, Département de Chimie, Faculté des Sciences, Université de Sherbrooke, 3001, 12e Avenue Nord, Sherbrooke, Québec, J1H 5N4 (Canada)

‡Institut de Pharmacologie de Sherbrooke, Département de Chirurgie/Urologie, Université de Sherbrooke, 3001, 12e Avenue Nord, Sherbrooke, Québec, J1H 5N4 (Canada)

ABSTRACT

PACE4, a serine endoprotease of the proprotein convertases family, has been recognized as a promising target for prostate cancer. We previously reported a selective and potent peptide-based inhibitor for PACE4, named the multi-Leu peptide (Ac-LLLLRVKR-NH_2 sequence), which was then modified into a more potent and stable compound named C23 with the following structure; Ac-DLeu-LLLRVK-Amba (Amba: 4-amidinobenzylamide). Despite improvements in both in vitro and in vivo profiles of C23, its selectivity for PACE4 over furin was significantly reduced. We examined other Arg-mimetics instead of Amba to regain the lost selectivity. Our results indicated that the replacement of Amba with 5-(aminomethyl)picolinimidamide (Ampa) increased affinity for PACE4, and restored selectivity. Our results also provide a better insight on how structural differences between S1 pockets of PACE4 and furin could be employed in the rational design of selective inhibitors.

INTRODUCTION

There is substantial evidence that proprotein convertases (PCs) are broadly involved in the malignancy of tumors and angiogenesis.[1] This family of serine endo-proteases consists of seven members namely PC1/3, PC2, furin, PACE4, PC4, PC5/6 and PC7, which process their substrates at the consensus motif of R-X-R/K-R-↓-X, X being any amino acid residue.[2] The role of PCs in malignancies is through the activation proteolysis of oncogenic precursor proteins. Among these substrates, growth factors and their receptors (e.g, transforming growth factor-β and insulin-like growth factor-1 receptor family members) are crucial for cell growth. Other PC substrates, such as proteases from ADAM (a Disintegrin and metalloproteinase) and MMP (Matrix-metalloprotease) families, as well as adhesion molecules (e.g. E-cadherin) are crucial for cell adhesion and metastasis.[3] Additionally, the list of substrates includes other regulatory proteins, along with bacterial and viral toxins.[4]

The cellular overexpression of PCs provides a clue for their role in tumorigenesis, as observed in many malignant cell types.[5] This is the case for PACE4 which is

overexpressed in prostate cancer (PCa) and other cancer cell lines.[6-10] mRNA silencing studies demonstrated that inhibition of PACE4 had effects on tumorigenesis and neovascularization PCa cell line and animal models.[11] More recently, pro-growth differentiation factor-15 (pro-GDF-15) was identified as a PACE4 specific substrate in PCa involved in the proliferative phenotype. A PACE4 isoform, known as PACE4-altCT is overexpressed in PCa cell lines has been found to be responsible for sustained tumor progression.[12] It is clear that PACE4 inhibition could open a new therapeutic strategy for PCa either as mono or co-therapy, thus justifying our increased efforts to develop clinically relevant PACE4 inhibitors.

In a previous study, we showed that a lipophilic tail composed of four leucine residues attached to the N-terminus of the RVKR tetrapeptide, was critical to increase the selectivity of PACE4 inhibitors. Thus, our octapeptide, named multi-Leu (compound **1**), inhibits PACE4 and furin with K_i = 22 and 430 nM, respectively (**Figure 1**).[13] The replacement of P1-Arg with 4-amidinobenzylamide (Amba) and P8-Leu with its D isomer resulted in our current lead, named C23 (compound **2**;

Figure 1), with improved PACE4 affinity (K_i = 4.9 nM). Whereas the multi-Leu peptide **1** was rapidly metabolized when tested in vivo, C23 was much more stable and consequently displayed prominent pharmacological efficiency (IC_{50} = 25 and 45 µM for DU145 and LNCaP PCa cells, respectively) with rapid uptake by xenografted tumors, and a human plasma half-life of 1.7 h.[11, 14] However, Amba develops stronger interactions with the furin S1 pocket than the C-terminal Arg residue in compound **1**, resulting in a significant reduction in selectivity (only 2-fold) for PACE4 over furin. The furin preference for P1-Amba is even more visible with the tetrapeptide Ac-RVK-Amba. This simple ligand is twice as selective toward furin, emphasizing the undeniable role and necessity of the four leucine-tail for PACE4 selectivity.[15]

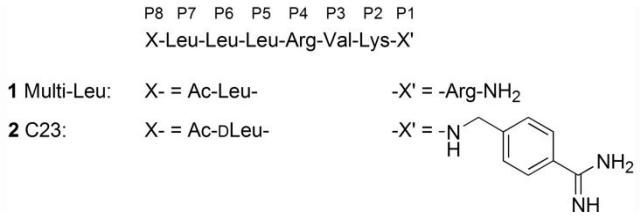

Figure 1. Structure of control PACE4 inhibitors **1** and **2**.

In another study, we successfully improved the selectivity of the multi-Leu peptide by introducing β-branched basic residues in the P3 position. This led to a 40-fold selective inhibitor.[16] However, further studies determined that this type of compound, harboring four consecutive basic residues, was devoid of PCa cells antiproliferative activity, suggesting a lack of cell penetration to reach the PACE4-altCT intracellular target. Trials to improve the selectivity of C23 by manipulating its P5-P8 portion met with limited success (3-fold selectivity in favor of PACE4). All these data reveal that the Amba residue constitutes a barrier for achieving more selective compounds.[17] This work relates our efforts to find alternative residues that could successfully replace Amba at the P1 position.

Homology models of PACE4 suggest that the S1 pocket, which accommodates the P1 residue of the inhibitors, is constructed from two remote regions (primary structure): The first one described as a β-sheet then loop motif runs from S305 to G319 and the second one, a loop-helix-loop, encompasses residues S345 to I364. These two parts of the cleft are clamped together by means of several interactions including a Ca^{2+} cation involved in salt bridges with D310, D353,

D358 and E381 (**Figure 2**).[18] The guanidinium ion of the P1 residue (Ac-RVK**R**-NH_2) is strongly held inside the S1 pocket by means of ionic forces with aspartates 310 and 358, as well as ion-dipole interactions with the carbonyl groups of P308 and A344. These interactions are identical within all PCs.[18] However, despite the high degree of homology in and around the S1 pocket, differences exist, as observed in the matching sequences ^{300}**H**D**S**C**N** and ^{352}**G**D**Y**C**S** of furin and PACE4, respectively (see **Figure 2**). One hypothesis is that these disparities, that concern three residues only, alter the shape of the S1 pocket in furin and PACE4 and may be responsible for the observed selectivity differences between compounds **1** and **2**.

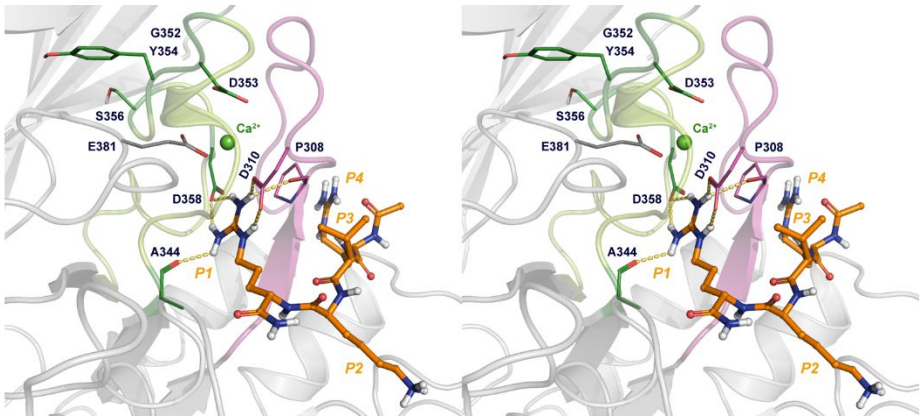

Figure 2. Stereo representation of a PACE4 P1-P4 active site homology model with docked Ac-RVKR-NH_2 (orange) inhibitor. The Ca^{2+} cation (green sphere) located deep inside the S1 subsite is essential for its stability.

Generally, refining the selectivity is more laborious than enhancing potency,[19] and given the high degree of homology between furin and PACE4, discrimination between these two enzymes is challenging. Although C23 is highly potent in blocking tumor progression of xenograft PCa animal models, inhibition of the most ubiquitous member of the PC family, furin, could potentially lead to unforeseen side effects and drawbacks. In the present study, new residues are rationally designed, then introduced in the P1 position, based on available structural data and structure activity relationship (SAR) studies conducted on both PACE4 and furin. The main goal of our investigations is to determine the structural factors (P1 position) that might discriminate between PACE4 and furin, in order to create potent and selective PACE4 inhibitors.

RESULTS AND DISCUSSION

Design and binding affinities. Two groups of mimetics were designed (and biologically tested: PACE4 and Furin K_i, DU145 and LNCaP cell lines IC_{50})[13, 20] for the P1 residue of PACE4 inhibitors (**Figure 3**): a) an aliphatic series in which inhibitors **3**-**6** possess a guanidine group like Arg itself; and b) an aromatic series whose members **7**-**13** bear an amidine function like Amba. Compound **3** is an epimer of **1** at position P8. Both compounds have similar K_i values, but **3** is more selective (PACE4 K_i = 24 nM, 32 times selective for PACE4). The D residue at position P8 imparts metabolic stability and this is likely the reason why **3** is endowed with an improved ability to inhibit PCa cell proliferation. Accordingly, all newly synthesized inhibitors discussed in this work have a DLeu residue at position P8, like compounds **2** and **3**.[20] The first two derivatives **4** and **5** were rigidified analogs of **3**, from which the terminal amide had been removed (agmatine). The alkene **4** proved to be much better than the alkyne **5**.[14] The improved affinity of **4** (K_i = 13 nM), compared to compound **3**, however was associated with substantial reduction of selectivity (3-fold for PACE4). Conversion of the C-terminal amide to an alcohol moiety in **6** resulted in a poor and non-

selective inhibitor of PACE4. These observations are, however, consistent with the poor inhibition of peptide alcohols reported for other serine proteases.[21-22]

Together with the Amba derivative **2**, the compounds **7** and **8** were used to carry out a preliminary SAR study of the aromatic amidine. Contrary to the Arg analogs **3**-**6**, the side chain of Amba is more rigid and it is also bulkier.[18, 23] It is anticipated that the amidine group will be held in the S1 pocket by the same enzyme residues that interact with the equivalent guanidine of Arg (**Figures 2** and **5**). As can be observed, P308 and A344 carbonyls, and D310 and D358 carboxylates bind tightly to the two external NH_2 parts of the guanidinium ion. Additionally, D310 can develop an extra interaction with the arginine delta-NH, so any designed mimics ideally need an equivalent hydrogen bond donor.

First, the analogues **7** and **8** were designed to assess the width and length of the S1 pocket. Further extension of Amba with one methylene unit, producing inhibitor **7**, not only did not offer any improvement in selectivity, but also reduced the binding affinity (PACE4 K_i = 17 nM). The tetra-fluorinated Amba derivative **8** has very little affinity toward PACE4 and furin. There are two possible explanations

for this negative result: Either the S1 pocket is too narrow to accommodate the four fluorine atoms or the positive charge is lacking since the calculated pK_a of the tetrafluoro-benzamidine is as low as 6.9.[24]

According to plans, O and NH substituents were introduced at the ortho position of the benzamidine, inside a fused 5-membred ring as in **9** and **10** respectively, then as free phenol **11** and aniline **12**. Finally, the pyridine **13** was designed as a more direct mimetic of **2**, since it could fill up the same space in the S1 pocket. The inhibitor candidates **9-13** were synthesized then tested biologically. The bicyclic systems **9** and **10** proved essentially inactive; whereas, the *Ki* values of the corresponding open systems, **11** and **12**, are in the same range as those of multi-Leu **1** and its diastereomer **3**, albeit with lower selectivities. Whereas, compound **13** is indeed a strong and selective inhibitor (K_i = 2.6 nM, PACE4). The P1 residue of compound **10** has been recently used in P1 of furin inhibitors with no success.[25]

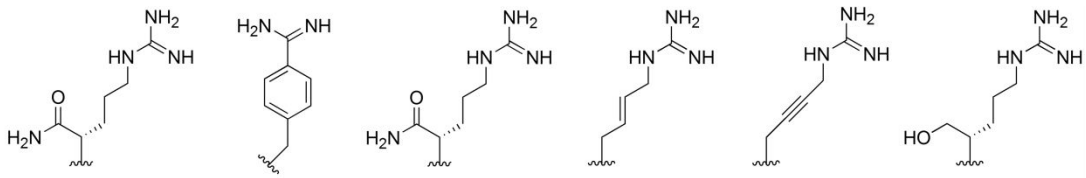

	1[a] Multi-Leu	2[b]	3[b]	4[b]	5	6
PACE4 K_i (nM):	22 ± 6	4.9 ± 0.9	24 ± 2	13 ± 3	32 ± 4	190 ± 30
Furin K_i (nM):	430 ± 10	9.8 ± 2	760 ± 20	38 ± 4	60 ± 10	250 ± 30
Selectivity:	20	2	32	3	2	9
DU145 IC_{50} (μM):	100 ± 10	25 ± 10	70 ± 30	40 ± 10	110 ± 30	N.C.[c]
LNCaP IC_{50} (μM):	180 ± 10	40 ± 10	150 ± 40	210 ± 20	125 ± 10	N.C.

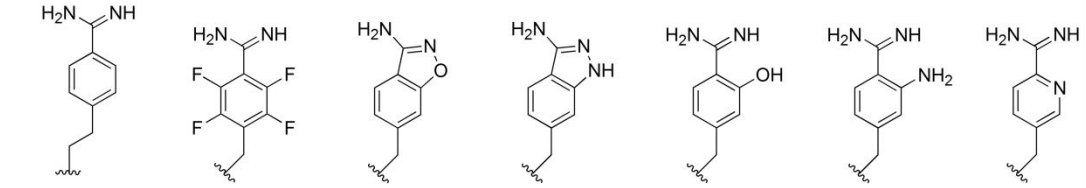

	7	8	9	10	11	12	13
PACE4 K_i (nM):	17 ± 3	240 ± 20	500 ± 130	700 ± 50	53 ± 7	14 ± 4	2.6 ± 0.1
Furin K_i (nM):	41 ± 3	600 ± 100	614 ± 2	825 ± 10	240 ± 20	60 ± 10	21.5 ± 0.9
Selectivity:	2	2	1	1	5	4	8
DU145 IC_{50} (μM):	80 ± 10	69 ± 7	N.D.[d]	N.D.	50 ± 10	61 ± 7	130 ± 20
LNCaP IC_{50} (μM):	80 ± 6	230 ± 50	N.D.	N.D.	113 ± 1	58 ± 7	140 ± 10

Figure 3. Structure of P1 arginine mimetics used for PACE4 inhibitors with general structure of Ac-DLeu-Leu-Leu-Leu-Arg-Val-Lys-NHR apart from **1** [a]with Leu at position P8 instead of DLeu.[13] The inhibition of PACE4 and furin are represented as K_i ± SD, and antiproliferative activity on PCa cell lines as IC_{50} ± SEM. [b]Data adapted from Ref. 14; [c]Not calculable, indicates that the curve did not converged to 50% with doses up to 150 μm; [d]Not determined, due to solubility/precipitation problems.

In order to provide a rationale for the various K_i values, that are linked to the mode of binding of the P1 side chains, DFT calculations were run (**Figure 4**).[26] These calculations were intended to disclose the minimum energy conformations

of Amba derivatives and other relevant properties. The pK_a figures of the amidinium ions and ortho functional groups were also estimated.[24] It was first confirmed that the rigid Amba (side chain in **Figure 4b**) is indeed a good mimic of Arg (**Figure 4a**). For these two P1 residues, the distances between the Cα and the central cation C atoms are 6.24 Å and 5.78 Å for Arg and Amba respectively (**Figure 5**). Amba, being slightly shorter, can fit in the S1 cavity without much distortion. This does not hold true for the longer Amba analog **7**, as demonstrated by its lower affinity (17 nM). In terms of charges, both guanidine and amidine are also similar since they exist as guanidinium and amidinium cations at physiological pH. By incorporating these functional groups in rings through addition of O and NH atoms, the resulting bicyclic systems (**Figure 4c** and **4d**) are fully aromatic. Consequently, their N atoms are no longer basic (pK_a: 1.0-3.5) and are not positively charged at physiological pH. As for compound **8** (mostly neutral at pH 7.4), which suffered the same drawback, the affinities of analogs **9** and **10** are drastically diminished. Upon breaking the N-O and the N-N bonds of their heterocycles, the amidine moiety becomes strongly basic (**Figure**

4e and **4f**) and the corresponding peptidomimetics **11** and **12** recover some inhibitory activity, the aniline **12** being much stronger than the phenol **11** (**Figure 3**). Calculations show that at physiological pH (7.4), the phenolate anion is the predominant species. Since a negative charge in that region of the inhibitor may lead to unfavorable interactions with the carboxylate of D310 (**Figures 5**), this may easily account for the lower affinity of inhibitor **11** for both furin and PACE4. In addition, the introduction of the aniline and phenol groups increases steric hindrance in the deep S1 subsite and may explain why both **11** and **12** are less potent than **2**.

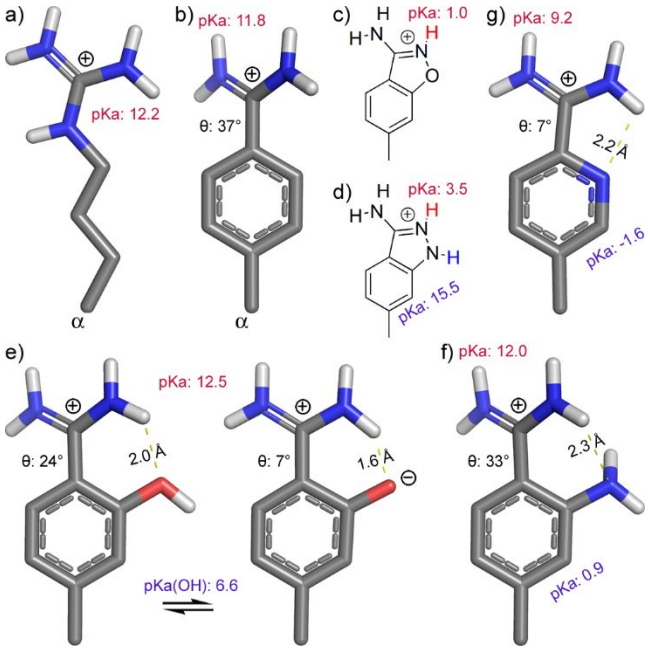

Figure 4. Energy-minimized (DFT) side chain conformers of arginine (**a**) and arginine mimetics (**b**, **e**-**g**) and estimated pK_a values of relevant functional groups. Torsion angles between amidine and aromatic planes are shown (θ).

Despite its additional NH_2 group, the aniline (**Figure 4f**) is geometrically very close to its parent amidine devoid of substituents (**Figure 4b**). For both cases, the amidinium plane is rotated relative to the aromatic ring by ~ 35°. Surprisingly, this torsion angle is smaller in the case of the aniline, because of its ortho position that induces the formation of an intramolecular hydrogen bond N−H···N. However, for obvious steric reasons, the aniline-substituted amidine is prevented from reaching a fully flat geometry, contrary to the simpler amidine that can, at a cost of 2.8 kcal.mol^{-1} according to DFT calculations. The K_i values (PACE4) for the corresponding inhibitors **2** and **12** are 4.9 nM and 14 nM, respectively (**Figure 3**).

The best compound of the whole series is the pyridine **13**, in terms of affinity for PACE4 (2.6 nM) as well as selectivity (8 for compound **13** compared to only 2 for compound **2**). This overall beneficial effect does not arise from a better

electronic complementarity with D310, because the pyridine nucleus is so electron-deficient that it is not basic at all (pK_a: -1.6, **Figure 4g**) and remains neutral at all pHs. Nevertheless, the lone pair of the pyridine is ideally positioned for an intramolecular hydrogen bond N···H−N with the neighboring amidinium partner. As a result, the terminal side chain of **13** is very flat indeed, its torsion angle θ is as small as 7°, a significant gain of 30° by comparison with isosteric peptide mimic **2** (see **Figure 4b** and **4g**). Induced-fit docking models (**Figure 5**) suggest that the pyridine N atom makes no additional interaction with PACE4, in which case its sole purpose is to freeze the amidinium side chain in its flat conformation. From all these results, it can be inferred that a planar conformation of the P1 residue might fit better in PACE4 S1 pocket compared to furin.

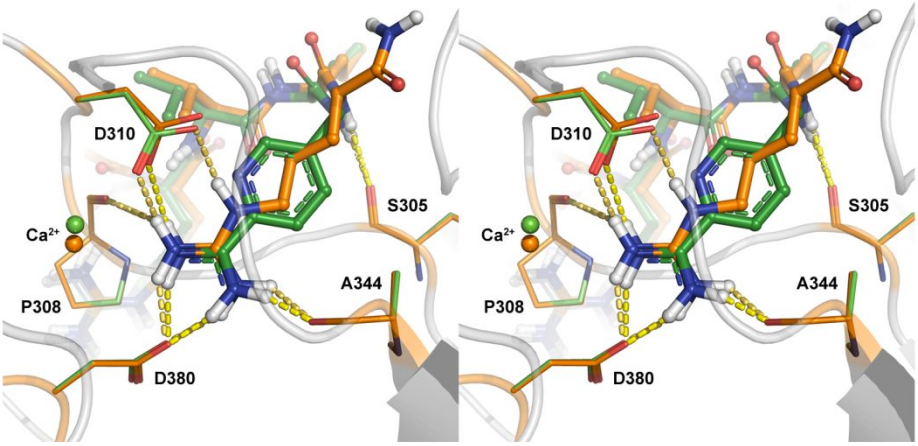

Figure 5. Superimposed *induced fit docking* pose of Ac-RVKX corresponding to the P5-P1 region of compounds **1** (orange) and **13** (green) in the PACE4 homology model active site.[18] Enzyme's side chain C atoms colored the same as corresponding ligand for clarity. H, N and O atoms are in white, blue and red color, respectively. Hydrogen bonds are represented as yellow dashes.

Cell-based assays. In order to evaluate the cell antiproliferative activities, the inhibitors were tested against PCa cell lines (DU145 and LNCaP) using an MTT proliferation assay **(Figure 3**). In terms of cell-based efficacy, neither compounds **4** nor **5** showed significant advantage over compound **3** despite their differences in PACE4 affinity and selectivity. However, the poor affinity of inhibitor **6** for PACE4 entirely translated into antiproliferative activity, and no effect was observed on both cell lines for this inhibitor in concentrations below 150 μM further depicting the relationship between the anti-proliferative response and PACE4 inhibition. Inhibitors **9** and **10**, precipitated during the assay and, thus, their IC_{50} values were not measurable.

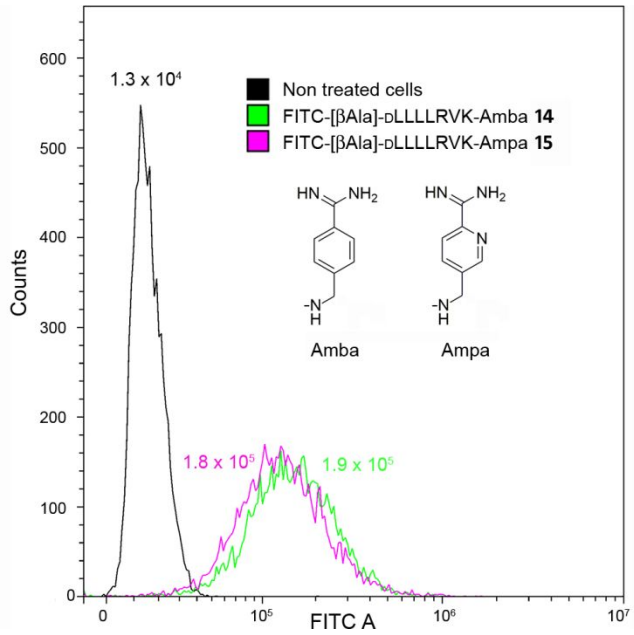

Figure 6. Cell permeability comparison of FITC-labeled analogues **14** and **15** of compounds **2** and **13**.

Analogues **7**, **8**, **11** and **12** which are less potent PACE4 inhibitors compared to the parent compound **2**, displayed inferior antiproliferative activity (**Figure 3**). Whilst still active, inhibitor **13** (IC_{50} = 130 and 140 μM for DU145 and LNCaP cells, respectively) displayed lower antiproliferative activity than control compound **2** (IC_{50} = 25 and 45 μM for DU145 and LNCaP cells, respectively). Knowing the requirements of PACE4 inhibition to reach the intracellular PACE4 for efficient antiproliferative activity, the cell permeability of **13** was tested using its N-terminally FITC labelled version (compound **15**).[13,14,27] However, the results depicted no

considerable difference in its permeability compared to the control FITC-labeled analogue **14** corresponding to inhibitor **2** (**Figure 6**).

Overall, compound **13** with the best affinity for PACE4 and reasonable selectivity among the P1 modified inhibitors provided reasonable antiproliferative activity in PCa cell lines. The Ampa could be an appropriate P1 residue for further development of more selective PACE4 inhibitors.

Chemistry. All the peptides **5** and **7−13** were synthesized using a combination of solid and solution phase peptide synthesis as reported earlier for compound **2**.[14] Briefly, the fully-protected P8-P2 peptide was synthesized with conventional Fmoc-*t*Bu strategy on 2-chlorotrytylchloride resin. After coupling of the last amino acid and removal of the Fmoc protective group, the peptide was acetylated, then cleaved from resin under mild acidic conditions. The P1 residue amines were then coupled with the protected peptide in solution. The fragment coupling procedure used to connect the heptapeptide to arginine mimetic synthons may obviously lead to some degree of epimerization at the P2 position, the lysine residue. However, the final products were proven to be pure by 1H NMR

spectroscopy after reverse phase preparative HPLC. Compound **6** was prepared in a different manner using a literature method for the synthesis of C-terminal alcohol peptides.[28] In the final step, the side chains of all the peptides, were deprotected using TFA cocktails. The FITC-labeling of compound **15** was carried out as previously reported for compound **14**.[14]

The alkyne **18**, P1 residue of compound **5**, was obtained from two consecutive Mitsunobu reactions on 2-butyne-1,4-diol **16** and a final phthalimide deprotection (**Scheme 1**). For the P1 residues of **9** and **10**, compound **19** was converted to a dinitrile **20**. The regioselective formation of 5-membered ring, was followed by reduction of the remaining nitrile moiety to yield compounds **21** and **22**. The inhibitor **11** was then prepared by catalytic hydrogenation of inhibitor **9**.

Scheme 1. Synthesis of P1 arginine mimetics 18, 21 and 22 for inhibitors 5, 9 and 10 [a]

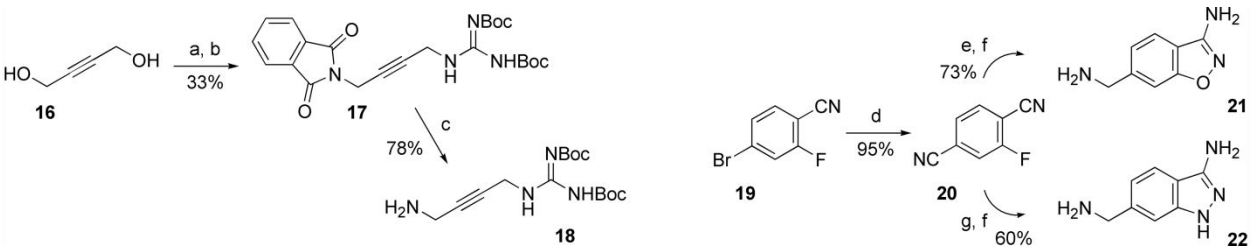

[a]Reagents and conditions: (a) phthalimide, DIAD, PPh_3, THF, 0 °C to rt, 16 h; (b) *N,N'*-Di-Boc-guanidine, DIAD, PPh_3, THF, 0 °C to rt, 16 h; (c) $N_2H_4.H_2O$, $CHCl_3$/MeOH, 4 h; (d) $Pd(PPh_3)_4$, $Zn(CN)_2$, DMF, 80 °C, 6 h; (e) AcNHOH, K_2CO_3, DMF, 12 h; (f) BH_3-THF 1 M in THF, 0 °C to rt, 6 h; (g) $N_2H_4.H_2O$, *n*-BuOH, reflux, 16 h.

The synthetic pathways of four other P1 residues are outlined in **Scheme 2**. Compound **25** was obtained by condensation of 4-formylbenzonitrile **23** with nitromethane prior to consecutive reduction of the double bond and nitro group, then Boc protection of the resulting amine giving compound **25**. The nitrile group of this compound was then converted to an amidine and the Boc protection was removed to afford compound **26**.[29] Nitromethane was also employed in a S_NAr2 reaction to prepare **28** from pentafluoro-benzonitrile **27**. The nitro product **28** was transformed to the Arg mimetic **29** by conversion of nitrile to amidine. The final step of the conversion to **29** included a catalytic reduction which the nitromethyl moiety was reduced to the aminomethyl as well. The benzylic alcohol **31** was prepared by oxidation of the methyl substituent in the starting material **30**. The

alcohol **31** was transformed into the corresponding tosylate, then azide, which was finally converted to the Boc-protected amine **32** via a Staudinger reaction. The nitrile of **32** was transformed into an amidine as before (**25** to **26**), during which process the nitro group was also reduced to an aniline (step f in **Scheme 2**). Cleavage of the Boc group yielded the amine **33**. The bromide in **34** was replaced by a nitrile, then its ester was reduced to the benzylic alcohol **35**. Mitsunobu reaction on **35**, using phthalimide as nucleophile, followed by hydrazine opening of the resulting phthalimide led to the corresponding amine, that was immediately protected as its *t*-butyl carbamate **36**. From there, the same three-step procedure used to prepare **26** from **25**, and **29** from **28**, was applied to **36** to obtain the amine **37**.

Scheme 2. Synthesis of P1 arginine mimetics 26, 29, 33 and 37 for inhibitors 7, 8, 12 and 13[a]

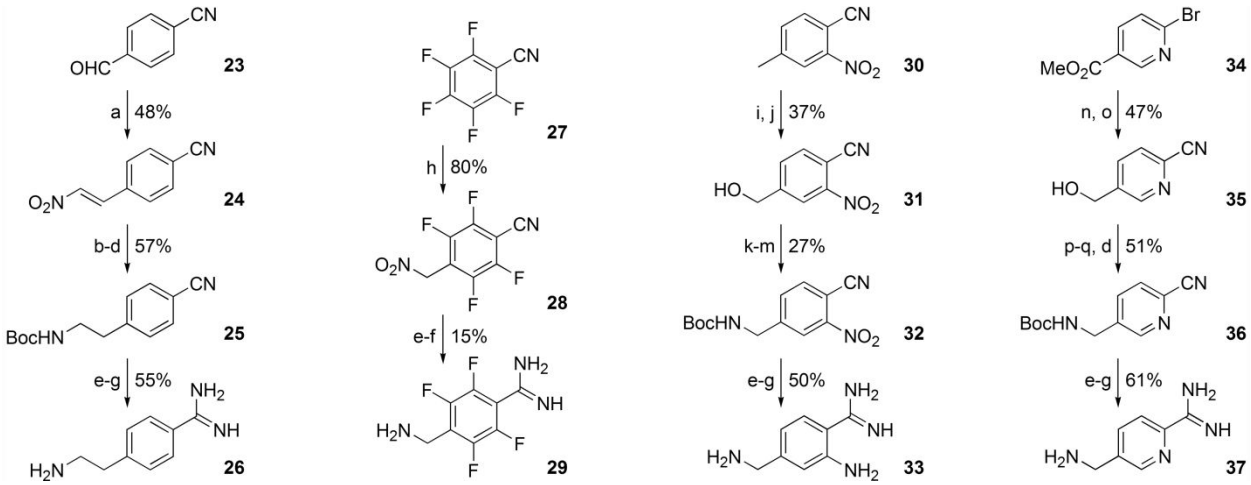

[a]Reagents and conditions: (a) $MeNO_2$, NaOH, MeOH/H_2O, <10-15 °C, 15 min then 5 M HCl; (b) Bu_3SnH, CH_2Cl_2, rt, 16 h; (c) Zn, HCl(aq), 65 °C, 1h; (d) $(Boc)_2O$, K_2CO_3, THF/H_2O, 16 h; (e) $NH_2OH.HCl$, DIPEA, MeOH, 60 °C, 16 h; (f) Ac_2O, DIPEA, THF then 10% Pd/C, AcOH/MeOH, 35 psi H_2, 12 h; (g) Conc. HCl(aq), MeOH, 0 °C to rt, 1 h; (h) $MeNO_2$, TMG, -35 °C, 5 min; (i) H_5IO_6, CrO_3, MeCN, 3 h; (j) *i*-BuOCOCl, NMM, THF, 0 °C, 2 min then $NaBH_4$ in MeOH, 30 min; (k) TsCl, Et_3N, DMAP, MeCN, 1 h; (l) NaN_3, NaI, DMF, 1 h; (m) PPh_3, H_2O, THF, 16 h then K_2CO_3, $(Boc)_2O$, 16 h; (n) $Pd(PPh_3)_4$, $Zn(CN)_2$, DMF, 100 °C, 16 h; (o) $NaBH_4$, LiCl, MeOH, 2 h; (p) phthalimide, DIAD, PPh_3, THF, 0 °C to rt, 16 h; (q) $N_2H_4.H_2O$, $CHCl_3$/MeOH, 3 h.

CONCLUSION

In conclusion, we developed new inhibitors for PACE4 through SAR studies of the P1 residue. Our results emphasize structural differences in the S1 pocket that can be used to discriminate between furin and PACE4. This could open a novel avenue for achieving higher selectivity. Inhibitor **13** is the most potent and selective inhibitor in the series and displayed K_i = 2.6 nM which is 2-fold more potent and 4-fold more selective than C23 (compound **2)**. Although the P1-Ampa in **13** introduces the same stabilizing Van der Waals contacts as Amba in **2**, the former is held rigidly (intramolecular H bond) in a flat conformation, suggesting that its gain in affinity for PACE4 might precisely results from this rigidifying process. Despite similarities in structures and cell permeabilities, surprisingly, compound **13** exhibited lower efficiency in PCa cell antiproliferative assay compared to **2**. Further studies may provide the knowledge to explain this impairment, however, this significant improvement at the P1 position can now be used in combination with other modifications at other positions.

EXPERIMENTAL

Chemistry. All chemical reagents and solvents were obtained from commercial resources and used without further purification. Fmoc-protected amino acids and coupling reagents, were purchased from ChemPep (Miami, FL, USA) or Chem-Impex International (Wood Dale, IL, USA), and 2-chlorotrityl-chloride resin from Rapp Polymer (Tübingen, Germany). Other reagents were purchased from Sigma Aldrich (St. Louis, MO, USA). Manual Fmoc/tBu strategy was utilized for peptide synthesis. Analytical reverse phase high-performance liquid chromatography (RP-HPLC) was performed on an Agilent Technologies 1100 system equipped with a diode array detector (λ = 210, 214, 230, and 254 nm). Preparative HPLC were accomplished on a Waters preparative HPLC machine (Autosampler 2707, Quaternary gradient module 2535, UV detector 2489 (λ = 214 and 230 nm), fraction collector WFCIII) equipped with an ACE5 C18 column (250 × 21.2 mm, 5 µm spherical particle size). Analytical HPLC was carried out using C18 columns, either Agilent Eclipse XDB (5 mm, 4.6 µm, 250 mm) or a Phenomenex Jupiter (5 mm, 4.6 µm, 250 mm). A gradient of H_2O/MeCN containing 0.1% TFA was used as eluent for both analytical and preparative HPLC. The identity of the pure

products was confirmed using an ESI-HRMS system (TripleTOF 5600, ABSciex; Foster City, CA, USA). For synthesis check a Water H Class Acquity UPLC coupled with an SQ Detector 2 and a PDA eλ detector paired with an Acquity UPLC CSH C18 column (1.7 µm × 2.1 mm × 50 mm) was used with a linear gradient from 5 to 95% of MeCN containing 0.1% formic acid in 0.1% aqueous formic acid was used for 1.3 min and a flow rate of 0.8 mL/min. NMR experiments were carried out on either AV300 Bruker (300 MHz for ^{1}H and 75 MHz for ^{13}C) or Avance III hd 400 Bruker (400 MHz for ^{1}H, 377 MHz for ^{19}F and 100 MHz for ^{13}C) or Agilent Varian (600 MHz for ^{1}H) spectrometers. Complete decoupling of protons was applied in ^{13}C NMR experiments. The new compounds were additionally characterized by IR spectroscopy (Alpha-Platinum ATR Bruker, diamond crystal). The purity of biologically tested compounds **5–13** and **15** were confirmed to be more than 95% using reversed phase analytical HPLC and ^{1}H NMR (**13**). The compounds were characterized by HRMS.

Peptide synthesis general procedures. Compounds **5** and **7–10**, **12** and **13** were prepared as follows; Fmoc-Lys(Boc)-OH (1.2 equiv) was attached to 2-chlorotrityl

chloride resin in the presence of DIPEA (4 equiv) in DMF for 3h. The resin was washed using a sequence of DCM (3 ×), a cycle of MeOH/DCM (3 ×) and DCM (5 ×). The peptide chain was grown by standard Fmoc-SPPS. The Fmoc group was removed with 20% piperidine in DMF. The Fmoc protected amino acids were coupled using 5 equiv of protected amino acids, 5 equiv of HATU, and 15 equiv of DIPEA in DMF for 45 min. The last residue was acetylated by a solution of Ac_2O/DIPEA/DCM (5:10:85) for 30 min. Each protected peptide was released from the resin with a solution of 20% hexafluoro-2-propanol in DCM. The solvents were evaporated in vacuo, and the residue was lyophilized in *tert*-BuOH/H_2O (50:50). DIPEA (7.5 equiv) was added to an ice-cooled solution (0 °C) of protected peptide, arginine mimetic (2.5 equiv), PyBOP (2.7 equiv) and 6-Cl-HOBt (7.5 equiv) in DMF and the reaction stirred overnight at room temperature. The solvent was removed with an air stream to afford the crude protected peptide. The final deprotection of side chains was achieved by a solution of H_2O/TIPS/TFA (2.5:2.5:95) for 2 h. Purification with reversed phase preparative HPLC (gradients

of H_2O/MeCN containing 0.1% TFA) resulted in pure peptides as their TFA salts after lyophilization.

Compound 6. Fmoc-Arg(Pbf)-ol (0.63 g, 0.99 mmol)[30] was added to a 2% solution of DBU in DMF (7.0 mL) and agitated with 2-chlorotrytylchloride resin (0.3 g, 0.33 mmol) for 7 h. Fmoc-Lys(Boc)-OH (0.93 g, 1.98 mmol) was coupled to the free alcohol using DIC (0.15 mL, 0.99 mmol) and DMAP (0.01 g, 0.11 mmol). Then, the peptide was synthesized via deprotection/coupling cycles on resin as previously mentioned in the general procedure for peptide synthesis. After final acetylation, the protected peptide was obtained by treating the resin with 25% HFIP in DCM (5.0 mL). Solvents were removed and the O-N acyl migration was performed by stirring a solution of the resulting crude product in 20% piperidine in DMF (4.0 mL) for 1 h. Global deprotection was carried out as mentioned in the general procedure for peptide synthesis. The crude peptide was purified by preparative HPLC as described in the general procedure.

Compound 11. The peptide inhibitor **9** (0.05 g, 0.05 mmol) was dissolved in MeOH/H_2O (50:50, 4.0 mL). 10% Pd/C (50 mg) was added and the slurry was

stirred under H_2 (1 atm) for 16 h. After completion of the reaction (monitored by UPLC-MS), the reaction mixture was filtered through a pad of diatomaceous earth. The pad was washed with distilled water and the filtrate evaporated to dryness with a stream of air. The residue was purified by reversed phase preparative HPLC as described in the general procedure.

Compound 13. ^{1}H NMR (600 MHz, D_2O) δ (ppm): 8.64 (d, *J* = 1.8 Hz, 1H), 8.01 (d, *J* = 7.9 Hz, 1H), 7.94 (dd, *J* = 7.9, 1.8 Hz, 1H), 4.55 (AB d, *J* = 15.6 Hz, 1H), 4.49 (AB d , *J* = 15.6 Hz, 1H), 4.32-4.16 (m, 6H), 4.04 (d, *J* = 7.9 Hz, 1H), 3.14 (m, 2H), 2.96 (quin, *J* = 6.1 Hz, 2H), 2.01 (m, 1H), 1.97 (s, 3H), 1.86-1.70 (m, 4H), 1.70-1.49 (m, 16H), 1.45 (m, 1H), 1.37 (m, 1H), 0.92-0.80 (m, 30H).

***N*-(4-Phthalimido-but-2-ynyl)-*N′,N″*-1,3-bis(*tert*-butyloxycarbonyl)guanidine (17).** The first Mitsunobu intermediate product was obtained as a colorless solid in 52% yield using a reported procedure with all obtained spectra agreed with the literature.[31] ^{1}H NMR (400 MHz, $CDCl_3$) δ (ppm): 7.88 (dd, *J* = 5.4, 3.0 Hz, 2H), 7.75 (dd, *J* = 5.4, 3.0 Hz, 2H), 4.49 (s, 2H), 4.25 (br. s., 2H). ^{13}C NMR (100

MHz, $CDCl_3$) δ (ppm): 169.1, 134.2, 131.9, 123.5, 81.4, 79.2, 51.0, 27.2. HRMS-ESI (*m/z*): $[M + H]^+$ calcd for $C_{12}H_9NO_3$ 216.0665; found, 216.0653. The product (0.66 g, 3.1 mmol) was added to a solution of PPh_3 (0.78 g, 3.1 mmol), and 1,3-bis(*tert*-butoxycarbonyl)guanidine in dry THF (5.0 mL). The mixture was cooled in an ice bath and DIAD (0.5 mL, 3.1 mmol) was added dropwise and the reaction stirred for 16 h at room temperature under inert atmosphere. The residue was purified by flash chromatography (EtOAc/hexane) to give the title compound as a colorless solid (0.87 g, 63%). ^{1}H NMR (400 MHz, $CDCl_3$) δ (ppm): 9.36 (br. s., 1H), 9.14 (br. s., 1H), 7.88 (dd, *J* = 5.4, 3.0 Hz, 2H), 7.74 (dd, *J* = 5.4, 3.0 Hz, 2H), 4.74 (s, 2H), 4.44 (s, 2H), 1.48 (s, 9H), 1.47 (s, 9H). ^{13}C NMR (100 MHz, $CDCl_3$) δ (ppm): 167.0, 163.4,159.7, 154.2, 134.1, 132.0, 123.4, 84.5, 79.3, 79.0, 75.6, 34.4, 28.2, 27.8, 27.2. IR (neat) ν (cm^{-1}): 3381, 3279, 3246, 3029, 2978, 2941, 2358 (weak), 1728, 1686, 1604. HRMS-ESI (*m/z*): $[M + H]^+$ calcd. for $C_{23}H_{28}N_4O_6$ 457.2082; found 457.2068.

***N*-(4-Amino-but-2-ynyl)-*N′,N″*-1,3-bis(*tert*-butyloxycarbonyl)guanidine (18).** Compound **17** (0.71 g, 1.6 mmol) was dissolved in MeOH (12.0 mL) and $CHCl_3$

(9.5 mL), then 65% hydrazine monohydrate (1.0 mL) was added to the solution, that was stirred for 4 h. A white solid byproduct was filtered off. The filtrate was evaporated and diluted with $CHCl_3$ and then washed with 1 M aqueous sodium hydroxide. The organic phase was dried with magnesium sulfate, filtered and concentrated to give the desired product as a brownish solid (0.41 g, 78%). ^{1}H NMR (400 MHz, $CDCl_3$) δ (ppm): 9.36 (br. s., 1H), 9.14 (br. s., 1H), 4.73 (s, 2H), 3.39 (s, 2H), 1.52 (s, 9H), 1.47 (s, 9H). ^{13}C NMR (100 MHz, $CDCl_3$) δ (ppm): 163.4, 159.7, 154.3, 84.26, 78.9, 34.6, 31.5, 28.2, 27.9. IR (neat) ν (cm^{-1}): 3380, 2977, 2933, 2370 (weak), 1717, 1610. HRMS-ESI (*m/z*): $[M + H]^+$ calcd. for $C_{15}H_{26}N_4O_4$ 327.2027; found 327.2048.

2-Fluoroterephthalonitrile (20). A yellow slurry of 4-bromo-2-fluoro-benzonitrile **19** (1.00 g, 5.0 mmol), $Pd(PPh_3)_4$ (0.29 g, 0.25 mmol, 0.05 equiv) and $Zn(CN)_2$ (0.35 g, 3.0 mmol, 0.6 equiv) in deoxygenated dry DMF (6.5 mL) was heated at 80 ^oC for 6 h. The resulting solution was diluted with EtOAc and washed twice with 2 M ammonium hydroxide and brine. A yellow solid was obtained after flash chromatography with 15-20% EtOAc in hexane (0.70 g, 95% yield). ^{1}H NMR (400

MHz, $CDCl_3$) δ (ppm): 7.62 (dd, *J* = 1.4, 0.6 Hz, 1H), 7.60 (dd, *J* = 1.4, 0.6 Hz, 1H), 7.56 (dd, *J* = 1.4, 0.6 Hz, 1H). ^{13}C NMR (100 MHz, $CDCl_3$) δ (ppm): 162.9 (d, *J* = 260.0 Hz) 134.5, 128.5, 120.2 (d, *J* = 23.0 Hz) 118.4 (d, *J* = 10.0 Hz) 115.8 (d, *J* = 3.0 Hz) 112.1, 106.37 (d, *J* = 15.0 Hz). HRMS-ESI (*m/z*): $[M + H]^+$ calcd. for $C_8H_3FN_2$ 147.0353; found 147.0351.

6-(Aminomethyl)benzo[*d*]isoxazol-3-amine (21). Acetyl-hydroxamic acid (0.68 g, 9.0 mmol) was dissolved in DMF (12.0 mL). K_2CO_3 (2.21 g, 16.0 mmol) was added, followed by a few drops of H_2O. The mixture was stirred at room temperature for 30 min, then compound **20** (0.58 g, 4.0 mmol) was added. Stirring was continued for 12 h, water was added and the resulting mixture was extracted three times with EtOAc. The combined organic phases were dried over $MgSO_4$, filtered and evaporated in vacuum to give a colorless solid which was dissolved in dry THF (5.0 mL) and cooled in an ice bath. A 1 M solution of BH_3-THF in THF (12.0 mL, 12.0 mmol) was added dropwise and stirring was continued for 6 h. A 6 M HCl (15.0 mL) solution was added to the resulting white slurry and stirring was pursued for another 2 h. The solution was evaporated to dryness

and the residue purified by reverse phase HPLC to give the product as a colorless solid (0.48 g, 73% for two steps). ^{1}H NMR (300 MHz, D_2O) δ (ppm): 7.67 (d, *J* = 8.1 Hz, 1H), 7.42 (s, 1H), 7.26 (d, *J* = 8.1 Hz, 1H), 4.23 (s, 2H). ^{13}C NMR (75 MHz, D_2O) δ (ppm): 162.2, 159.0, 135.8, 123.5, 122.2, 116.3, 110.1, 42.9. HRMS-ESI (*m/z*): $[M + H]^+$ calcd. for $C_8H_9N_3O$ 164.08184; found 164.0819.

6-(Aminomethyl)-1H-indazol-3-amine (22). A mixture of **20** (0.60 g, 4.1 mmol) and hydrazine hydrate (0.6 mL, 12.3 mmol) in *n*-butanol (16.0 mL) was heated at reflux under inert atmosphere for 16 h. After completion of the reaction, the mixture was dried in vacuum and purified by flash chromatography (66 to 100% EtOAc in hexane as eluent) to yield brown crystalline needles (0.60 g, 93%). ^{1}H NMR (400 MHz, $CDCl_3$) δ (ppm): 11.96 (br. s., 1H) 7.88 (dd, *J* = 8.3, 1.0 Hz, 1H) 7.78 (t, *J* = 1.0 Hz, 1H) 7.21 (dd, *J* = 8.3, 1.0 Hz, 1H) 5.63 (s, 2H). ^{13}C NMR (100 MHz, $CDCl_3$) δ (ppm): 149.6, 139.7, 121.9, 119.8, 119.3, 115.7, 114.8, 108.1. This compound was treated with BH_3-THF, as was mentioned for compound **21**'s synthesis, to get **22** as a brownish solid (0.58g, 60%). ^{1}H NMR (300 MHz, D_2O) δ (ppm): 4.27 (s, 2H), 7.22 (d, *J* = 8.4 Hz, 1H), 7.47 (s, 1H),

7.81 (d, *J* = 8.4 Hz, 1H). ^{13}C NMR (75 MHz, D_2O) δ (ppm): 145.8, 142.5, 137.0, 122.3, 122.2, 112.1, 111.6, 43.0. HRMS-ESI (*m/z*): $[M + H]^+$ calcd. for $C_8H_{10}N_4$ 163.0978; found 163.0966.

(*E*)-4-(2-Nitrovinyl)benzonitrile (24). A solution of NaOH (0.84 g, 21.0 mmol) in ice-cold water (40.0 mL) was added dropwise to a solution of 4-formylbenzonitrile **23** (2.60 g, 20.0 mmol) and nitromethane (1.1 mL, 20.0 mmol) in MeOH (40.0 mL). The reaction temperature was kept below 10-15 °C during the addition of the NaOH solution. After stirring for 15 min, the whole reaction mixture was transferred to a separating funnel and slowly added to 5 M HCl (100.0 mL). A yellow solid was obtained almost instantly, it was filtered, washed with cold water, dried and recrystallized from hot EtOH to furnish the pure product **24** as yellow needles (1.66 g, 48%). ^{1}H NMR (400 MHz, $CDCl_3$) δ (ppm): 8.00 (d, *J* = 13.7 Hz, 1H), 7.77 (d, *J* = 8.4 Hz, 2H), 7.67 (d, *J* = 8.4 Hz, 2H), 7.62 (d, *J* = 13.7 Hz, 1H). ^{13}C NMR (100 MHz, $CDCl_3$) δ (ppm): 139.5, 136.5, 134.4, 133.0, 129.4, 117.8, 115.3.

***tert*-Butyl (4-cyanophenethyl)carbamate (25).** *n*-Bu_3SnH (2.4 mL, 8.9 mmol) was added to a solution of **24 (**1.29 g, 7.4 mmol) in dry DCM (19.0 mL) under inert atmosphere, and the reaction mixture was stirred for 16 h. The solvent was evaporated under reduced pressure, and the residue was partitioned between MeCN (100.0 mL) and hexane (30.0 mL). The MeCN phase was washed two times with hexane to remove the remained tin by-products and concentrated under reduced pressure. The residue was dissolved in MeOH (110.0 mL) and 2 M HCl (110.0 mL). Zinc powder (6.00 g, 90.0 mmol) was added slowly to the solution. After stirring for 1 h at 65 ^{o}C, the reaction mixture was cooled and basified to pH = 8 using sodium carbonate. The solid was filtered off, and the filtrate was concentrated to half of its volume. $(Boc)_2O$ (1.62 g, 7.4 mmol) in THF (50.0 mL) was added to the above solution and stirred for 16 h. THF was evaporated, and the resulting aqueous phase was extracted three times with EtOAc. The combined organic phases were washed with brine, dried over magnesium sulfate, filtered and evaporated to dryness. The residue was purified by flash chromatography (20% EtOAc in hexane as eluent) to furnish the title

compound as a colorless crystalline solid (1.13 g, 57% yield for three steps). ^{1}H NMR (300 MHz, $CDCl_3$) δ (ppm): 7.59 (d, *J* = 8.0 Hz, 2H) 7.30 (d, *J* = 8.0 Hz, 2H) 4.60 (br. s., 1H) 3.38 (q, *J* = 6.5 Hz, 2H) 2.86 (t, *J* = 6.5 Hz, 2H) 1.42 (s, 9H). ^{13}C NMR (75 MHz, $CDCl_3$) δ (ppm): 155.7, 144.7, 132.3, 129.6, 118.8, 110.3, 79.5, 41.3, 36.4, 28.3. HRMS-ESI (*m/z*): calcd. for $C_{14}H_{18}N_2O_2$ $[M + H]^+$ 247.1441; found 247.1415.

4-(2-Aminoethyl)benzimidamide (26). To a solution of **25** (0.27 g, 1.07 mmol) in MeOH (20.0 mL) was added hydroxylammonium chloride (0.11 g, 1.60 mmol) and DIPEA (0.28 mL, 1.60 mmol) and the reaction was stirred at 60 °C for 16 h. Then, the solvent was evaporated, and the residue was dissolved in EtOAc, washed with water and brine and dried over $MgSO_4$. The solvent was removed, and the residue was dissolved in THF (10.0 mL). DIPEA (0.28 mL, 1.60 mmol), and acetic anhydride (0.15 mL, 1.60 mmol) were added to the solution. The amidoxime intermediate was acetylated within 30 min as monitored by TLC. The excess of acetic anhydride was quenched by addition of H_2O (0.50 mL). Stirring was continued for 30 min. Then, the solvent was evaporated, and the residue

was dissolved in MeOH/AcOH (50:50) and 10% Pd/C (0.05 g) was added. The hydrogenation was conducted under 35 psi pressure of H_2 in a Parr hydrogenator jar for 12 h. Upon completion of the reaction (HPLC-MS), the mixture was filtered through a pad of diatomaceous earth and purified by preparative HPLC (gradient of 0 to 30% MeCN in water) to yield a colorless solid which was dissolved in MeOH (3.0 mL). Concentrated HCl (1.0 mL) was added slowly at 0 ^{o}C. After stirring for 1 h, the solvent was evaporated by an air stream overnight. The residue was resolubilized in a minimum amount of MeOH and triturated with Et_2O to give a colorless solid. ^{1}H NMR (300 MHz, D_2O) δ (ppm): 7.76 (dt, *J* = 8.0 Hz, *J* = 1.7 Hz, 1H) 7.51 (d, *J* = 8.0 Hz, 1H) 3.41 (t, *J* = 7.0 Hz, 1H) 3.09 (t, *J* = 7.0 Hz, 1H). ^{13}C NMR (100 MHz, DMSO-d_6) δ (ppm): 165.3, 144.0, 129.3, 128.4, 126.1, 39.2, 32.7 HRMS-ESI (*m/z*): calcd. for $C_9H_{13}N_3$ $[M + H]^+$ 264.1706; found 264.1683. The resulting solid was dissolved in MeOH (3.0 mL) in an ice bath (0 ^{o}C) followed by slow addition of conc. HCl (1.0 mL). The solvent was removed by an air stream after 1 h stirring. The residue was triturated using MeOH/Et_2O to furnish **26** as a white solid (55% for three steps). ^{1}H NMR (400

MHz, DMSO-d_6) δ (ppm): 9.34 (s, 2H), 8.40 (br. s., 2H), 7.87 (d, J = 8.4 Hz, 2H), 7.51 (d, J = 8.4 Hz, 2H), 3.00-3.09 (m, 4H). ^{13}C NMR (100 MHz, DMSO-d_6) δ (ppm) 165.3, 144.0, 129.3, 128.4, 126.1, 39.2, 32.7. HRMS (ESI) calcd for $C_9H_{13}N_3$ m/z $[M + H]^+$ 164.1182; found 164.1181.

2,3,5,6-Tetrafluoro-4-(nitromethyl)benzonitrile (28). Nitromethane (2.8 mL, 51.30 mmol) was placed in a flask and flushed with nitrogen for about 10 min, then 1,1,3,3-tetramethylguanidine (0.5 mL, 4.27 mmol) was added and the mixture stirred for 20 min. The mixture was cooled down to -35°C and pentafluorobenzonitrile (0.5 mL, 4.30 mmol) was slowly added. The reaction was stirred for 5 min and quickly quenched with 1 M aqueous HCl saturated with NaCl (10.0 mL). The solution was then extracted with EtOAc three times. The combined organic layers were washed with 0.1 M HCl then dried with magnesium sulfate, filtered and evaporated to give the desired product as a yellowish powder (0.80 g, 80%). ^{1}H NMR (400 MHz, $CDCl_3$) δ (ppm): 5.69 (s, 2H). ^{13}C NMR (100 MHz, $CDCl_3$) δ (ppm): 147.2 (m), 145.5 (m), 114.5 (t, J = 16.9 Hz), 106.6 (t, J = 3.7 Hz), 96.9

(t, J = 2.9 Hz), 65.5 (s). ^{19}F NMR (377 MHz, $CDCl_3$) δ (ppm): -137.2 (m, 2F), -130.5 (m, 2F). HRMS (ESI) calcd for $C_8H_2N_2O_2F_4$ m/z $[M + H]^+$ 235.0125; found 235.0143.

4-(Aminomethyl)-2,3,5,6-tetrafluorobenzimidamide (29). Compound **28** (0.60 g, 2.56 mmol) and hydroxylamine hydrochloride (0.27 g, 3.85 mmol) were added to a solution of DIPEA (0.7 mL, 3.85 mmol) in MeOH (40.0 mL), that was stirred gently overnight at room temperature. The mixture was extracted with ethyl acetate and the organic layer washed three times with saturated aqueous $NaHCO_3$ followed by brine, then dried with magnesium sulfate, filtered and evaporated in vaccuo. The obtained crude product (0.25 g, 0.95 mmol) and acetic anhydride (0.3 mL, 2.8 mmol) were added to a solution of acetic acid (5.0 mL) and the mixture was stirred for 1 h. Water (0.5 mL) was then added to the solution that was stirred for 1 h before addition of 10% Pd/C (0.08 g). After 48 h of stirring under hydrogen (balloon), the palladium was removed by filtration on diatomaceous earth and the solvents were evaporated in vaccuo. The product was purified by flash chromatography with 15% MeOH in DCM as eluent to furnish the title compound as a yellowish-brown oil (0.09 g, 15%). ^{1}H NMR (400

MHz, D_2O) δ (ppm): 5.69 (s, 2H). ^{13}C NMR (100 MHz, D_2O) δ (ppm): 156.8 (m), 144.6 (m), 142.7 (m) 122.2 (m), 113.1 (m), 32.7 (s). ^{19}F NMR (377 MHz, D_2O) δ (ppm): -141.0 (br. m, 2F), -139.8 (br. m, 2F). IR (neat) ν (cm^{-1}): 3566-2323 (br.), 1736, 1647, 1474. HRMS (ESI) calcd for $C_8H_2N_2O_2F_4$ m/z $[M + H]^+$ 222.0649; found 222.0661

4-(Hydroxymethyl)-2-nitrobenzonitrile (31). To a solution of H_5IO_6 (17.0 g, 75.0 mmol) in MeCN (300.0 mL) was added CrO_3 (0.30 g, 3.0 mmol) under vigorous stirring. Upon addition of 4-methyl-2-nitro-benzonitrile **30** (4.9 g, 30.0 mmol) to the above solution, a white precipitate formed. After 3 h of stirring, the supernatant liquid was decanted, and the solvent was removed by evaporation. The obtained product (2.7 g, 13.9 mmol) was dissolved in dry THF. The solution was cooled at 0 °C, isobutyl chloroformate (1.8 mL, 13.9 mmol) and NMM (1.5 mL, 13.9 mmol) were sequentially added with stirring. After 2 min, a solution of $NaBH_4$ (1.6 g, 41.7 mmol) in water (2.0 mL) was added to the above solution in one portion. The reaction mixture was stirred until gas evolution ceased (30 min), then it was quenched with a saturated NH_4Cl aqueous solution. The THF was evaporated from the reaction mixture in vacuum, and the residue was extracted

three times with EtOAc. The combined organic phases were dried over $MgSO_4$, filtered and the solvent was removed in vaccuo. Flash chromatography with EtOAc/hexane (40 to 50% EtOAc in hexane) afforded the pure product **31** as a colorless solid (2.0 g, 37% for two steps). ^{1}H NMR (400 MHz, DMSO-d_6) δ (ppm): 8.32 (s, 1H), 8.13 (d, *J* = 7.8 Hz, 1H), 7.89 (d, *J* = 7.8 Hz, 1H), 5.75 (br. s, 1H), 4.70 (d, *J* = 4.9 Hz, 2H). ^{13}C NMR (100 MHz, DMSO-d_6) δ (ppm): 150.5, 148.2, 135.6, 131.9, 122.6, 115.7, 104.7, 61.41. HRMS-ESI (*m/z*): $[M + H]^+$ calcd. for $C_8H_6N_2O_3$ 179.0451; found 179.0444.

***tert*-Butyl (4-cyano-3-nitrobenzyl)carbamate (32).** DMAP (0.06 g, 0.5 mmol) and triethylamine (1.7 mL, 12.0 mmol) were added to an ice-cooled solution of tosyl chloride (1.05 g, 5.5 mmol) and **31** (0.85 g, 4.8 mmol) in MeCN (10.0 mL). The reaction mixture was stirred for 1 h prior to evaporation of solvent. The residue was taken into EtOAc and washed with 0.5 M HCl and brine. The organic phase was then dried over $MgSO_4$, filtered and evaporated to dryness. The resulting solid was dissolved in DMF (10.0 mL). NaN_3 (0.94 g, 14.4 mmol) and NaI (0.36 g, 2.4 mmol) were added to the reaction mixture, that was stirred at room

temperature for 1 h. The reaction was quenched by addition of water, and the product was extracted with Et_2O (3 ×). The combined organic phases were dried over $MgSO_4$ and evaporated to dryness. The residue was purified by flash chromatography, using 20% EtOAc in hexane as eluent, to give a pale yellow oil (0.58 g, 60% for two steps). ^{1}H NMR (400 MHz, $CDCl_3$) δ (ppm): 8.31 (s, 1H), 7.95 (d, *J* = 8.0 Hz, 1H), 7.79 (d, *J* = 8.0 Hz, 1H), 4.65 (s, 2H). ^{13}C NMR (100 MHz, $CDCl_3$) δ (ppm): 142.9, 135.9, 132.9, 124.4, 114.6, 107.5, 53.1. HRMS-ESI (*m/z*): $[M + H]^+$ calcd. for $C_8H_6N_2O_3$ 204.0516; found 204.0513. The obtained 4-(azidomethyl)-2-nitrobenzonitrile (0.58 g, 2.9 mmol) was dissolved in a mixture of THF (10.0 mL) and H_2O (4.0 mL) and PPh_3 (0.76 g, 2.9 mmol) was added slowly to the solution. The mixture was stirred for 16h and its volume was reduced to one third of the original by evaporation. 2 M HCl was added to the residual aqueous solution, that was washed with EtOAc. The pH of the combined aqueous phases was adjusted to pH 8-9 by addition of solid K_2CO_3. A solution of $(Boc)_2O$ (0.62 g, 2.9 mmol) in THF (10.0 mL) was added to the above solution that was stirred for a further 16 h. THF was evaporated from the reaction mixture, and

the resulting aqueous phase was extracted to EtOAc (three times). The organic extract was dried ($MgSO_4$), the solvent was evaporated and the residue was purified by flash chromatography with 30% EtOAc in hexane to give a yellow oil which solidified at ambient temperature (0.36 g, 45%). ^{1}H NMR (400 MHz, $CDCl_3$) δ (ppm): 8.25 (s, 1H), 7.88 (d, *J* = 7.9 Hz, 1H), 7.74 (d, *J* = 7.9 Hz, 1H), 4.48 (d, *J* = 6.1 Hz, 2H), 1.47 (s, 10H). ^{13}C NMR (100 MHz, $CDCl_3$) δ (ppm): 155.8, 148.8, 146.9, 135.7, 132.5, 123.8, 114.9, 106.6, 80.7, 43.7, 28.3. IR (neat) ν (cm^{-1}): 3370, 3083, 2978, 2232, 1682, 1516, 1341, 1281. HRMS-ESI (*m/z*): $[M + H]^+$ calcd. for $C_{13}H_{15}N_3O_4$ 278.1135; found 278.1119.

2-Amino-4-(aminomethyl)benzimidamide (33). This compound was prepared from **32** with the same procedure that was used to get compound **26** from **25** (0.18 g, 50% yield for three steps). ^{1}H NMR (400 MHz, D_2O) δ (ppm): 7.39 (d, *J* = 8.0 Hz, 1H), 6.92 (d, *J* = 1.0 Hz, 1H), 6.87 (dd, *J* = 8.0, 1.0 Hz, 1H), 4.10 (s, 2H). ^{13}C NMR (100 MHz, D_2O) δ (ppm): 165.7, 145.3, 138.4, 130.1, 118.2, 117.4, 114.4, 42.5. IR (neat) ν (cm^{-1}): 3403-2602 (br.), 1738, 1637. HRMS-ESI (*m/z*): $[M + H]^+$ calcd. for $C_8H_{12}N_4$ 165.1135; found 165.1126.

5-(Hydroxymethyl)picolinonitrile (35). The cyanation of methyl 6-bromonicotinate **34** (1.30 g, 6.0 mmol) was accomplished as noted in the preparation of nitrile **20** from bromide **19**, except that the reaction mixture was heated at 100 °C for 16 h. The crude product was purified by flash chromatography (15% EtOAc in hexane) to give the intermediate cyanoester as a colorless solid (0.70 g, 64%). ^{1}H NMR (400 MHz, $CDCl_3$) δ (ppm): 9.30 (d, *J* = 1.0 Hz, 1H), 8.45 (dd, *J* = 8.0, 1.0 Hz, 1H), 7.81 (dd, *J* = 8.0, 1.0 Hz, 1H), 4.02 (s, 3H). ^{13}C NMR (100 MHz, $CDCl_3$) δ (ppm): 164.1, 151.8, 138.1, 137.0, 128.5, 128.1, 116.5, 53.1. HRMS-ESI (*m/z*): $[M + H]^+$ calcd. for $C_8H_6N_2O_2$ 163.0502; found 163.0489. The obtained solid (0.62 g, 3.8 mmol) was dissolved in MeOH (2.5 mL) prior to addition of LiCl (0.32 g, 7.7 mmol). Then, $NaBH_4$ (0.29 g, 7.7 mmol) was slowly added, and the reaction mixture was stirred for 2 h. The volatiles were removed from the reaction mixture by evaporation. The residue was treated with sat. aqueous NH_4Cl and extracted three times using EtOAc. The combined organic phases were dried over $MgSO_4$ and the solvent was removed in vacuum. The residue was purified with flash chromatography (50% EtOAc in hexane) to furnish the title compound

as a colorless solid (0.34 g, 73%). ^{1}H NMR (400 MHz, $CDCl_3$) δ (ppm): 8.71 (s, 1H), 7.89 (d, *J* = 7.9 Hz, 1H), 7.71 (d, *J* = 7.9 Hz, 1H), 4.86 (d, *J* = 5.2 Hz, 2H), 2.22 (t, *J* = 5.2 Hz, 1H). ^{13}C NMR (100 MHz, $CDCl_3$) δ (ppm): 149.5, 140.2, 135.0, 132.7, 128.3, 117.2, 61.9. HRMS-ESI (*m/z*): $[M + H]^+$ calcd. for $C_7H_6N_2O$ 135.0553; found 135.0538.

***tert*-Butyl((6-cyanopyridin-3-yl)methyl)carbamate (36).** 5-(Hydroxymethyl)picolinonitrile **35** (0.34 g, 2.5 mmol), PPh_3 (1.00 g, 3.8 mmol), and phthalimide (0.56 g, 3.8 mmol) were dissolved in dry THF (5.0 mL) under inert conditions and cooled at 0 ^{o}C in an ice bath. DIAD (0.75 mL, 3.8 mmol) was added by small portions over 30 min. The reaction mixture was stirred for 16 h at ambient temperature after which the solvent was removed in vacuo. The crude product was purified with flash chromatography. ^{1}H NMR (400 MHz, $CDCl_3$) δ (ppm): 8.81 (d, *J* = 2.0 Hz, 1H), 7.92 (dd, *J* = 8.0, 2.0 Hz, 1H), 7.89 (dd, *J* = 5.5, 3.0 Hz, 2H), 7.77 (dd, *J* = 5.5, 3.0 Hz, 2H), 7.67 (d, *J* = 8.0 Hz, 1H), 4.93 (s, 2H). ^{13}C NMR (100 MHz, $CDCl_3$) δ (ppm): 168.1, 151.9, 137.7, 136.2, 135.0, 133.8, 132.2, 128.5, 124.3, 117.4, 39.2. The phthalimide protecting group was

removed with the same procedure described for the preparation of **18** from **17**. The obtained solid was dissolved in H_2O (60.0 mL) and the pH was set to 8-9 using K_2CO_3. A solution of $(Boc)_2O$ (0.83 g, 3.8 mmol) in THF (30.0 mL) was added to the mixture that was stirred for 18 h. After evaporating one third of the solvent, the residue was extracted three times with EtOAc. The solvent was evaporated, and the residue purified by flash chromatography using 30% EtOAc in hexane to yield the title compound as a colorless solid (0.30 g, 51% for three steps). ^{1}H NMR (400 MHz, $CDCl_3$) δ (ppm): 8.65 (d, *J* = 1.4 Hz, 1H), 7.78 (dd, *J* = 7.9, 1.4 Hz, 1H), 7.68 (d, *J* = 7.9 Hz, 1H), 5.07 (br. s., 1H), 4.40 (d, *J* = 5.8 Hz, 2H), 1.46 (s, 9H). ^{13}C NMR (100 MHz, $CDCl_3$) δ (ppm): 155.8, 150.2, 138.9, 135.8, 132.6, 128.3, 117.1, 107.9, 80.5, 41.9, 28.3. IR (neat) ν (cm^{-1}): 3380, 2997, 2981, 2970, 2931, 2240, 1738, 1679, 1513. HRMS-ESI (*m/z*): $[M + H]^+$ calcd. for $C_{12}H_{15}N_3O_2$ 234.1237; found 234.1217.

5-(Aminomethyl)picolinimidamide (37). This compound was prepared using the same procedure that was used for compound **26** (0.12 g, 61% for three steps). ^{1}H NMR (300 MHz, D_2O) δ (ppm): 4.39 (s, 2H), 8.14 (d, *J* = 8.1 Hz, 1H), 8.20

(dd, *J* = 8.1, 1.0 Hz, 1H), 8.83 (d, *J* = 1.0 Hz, 1H). ^{13}C NMR (75 MHz, D_2O) δ (ppm): 162.3, 150.3, 144.3, 139.2, 133.8, 123.4, 40.1. IR (neat) ν (cm^{-1}): 3587-2629 (br.), 1672, 1650. HRMS-ESI (*m/z*): calcd. for $C_7H_{10}N_4$ $[M+H]^+$ 151.0987; found 151.0951.

DFT calculations. High-level DFT calculations (M06-2X/6.31Gdp)[26, 32, 33] was performed in water as solvent using GAMESS software (Version R1, 1 May 2013).[34]

Docking studies. Calculations were performed with the Molecular Operating Environment (MOE),[35] using a homology model of PACE4 developed from furin crystal structure (PDB code; 1P8J).[18,36] The Ac-RVKR-NH_2 was modified with the "*builder"* tool to the desired ligand and then minimized using the OPLS-AA force field. The general docking protocol of MOE (Receptor: *Receptor + Solvent*; Site: *Ligand Atoms*; Ligand: *Ligand Atoms*) was used for docking and the *Triangle Matcher* routine (Timeout: 300 s; Returned poses: 1000) as placement method. Acquired poses scored with the "*London dG"* algorithm (30 retained poses). The different poses were refined with the Induced Fit protocol (Refinement **>** Induced

Fit; Cutoff: 15 Å; Side Chains: Free; Termination Criterion: Gradient 0.01; Iterations: 500; Pharmacophore Restraint: Force Constant 100; Radius offset: 0.4) and rescored with the "*GBVI/WSA dG"* algorithm (5 retained poses). The docking score and the presence of vital interactions were used for the selection of best poses.

Enzyme kinetics. As reported earlier,[16] the PACE4 and furin inhibitory constants of compounds **5-13** were measured using Cheng and Prusoff's equation[37] and SoftMaxPro5 program except for compound **13**'s PACE4 affinity which was measured by Morrison's equation[38] and Prism 6.0 (GraphPad Software). All measurements were performed on a Gemini EM 96-well spectrofluorometer (Molecular Devices Sunnyvale, CA, USA) (λ_{ex} = 370 nm; λ_{em} = 460 nm; cutoff, 435 nm). The recombinant human furin ($[E_0]$ = 0.54 nM, K_m = 5.040 μM) and recombinant human PACE4 ($[E_0]$ = 20.18 nM, K_m = 4.035 μM) were prepared and purified as described before.[39] The competitive substrate was pGlu-Arg-Thr-Lys-Arg-AMC peptide (Bachem, Switzerland) for both furin and PACE4 with a concentration of 100 μM per well. Enzyme inhibition assays for furin were

performed in 100 mM Hepes pH 7.5, 1 mM $CaCl_2$, 1 mM β-mercaptoethanol, and 1.8 mg/mL BSA, while assays for PACE4 were performed in 20 mM Bis-Tis pH 6.5, 1 mM $CaCl_2$, and 1.8 mg/mL.

Cell proliferation assay. Cell lines were purchased from the American Type Culture Collection (ATCC) and maintained in RPMI-1640 and supplemented with 5% fetal bovine serum (FBS) for DU145 and 10% FBS for LNCaP. The antiproliferative activity of compounds **5-13** was evaluated as reported earlier.[13, 20] The IC_{50} values were calculated using Prism 6.0 (GraphPad Software).

Cell permeability. The DU145 cells were plated (200000 cells per 100 mm petri dish) and incubated for 48 h at 37 ^{o}C. After addition of a 1 μM solution of FITC-labeled analogs and further incubation for 1 h at 37 ^{o}C, cells were collected by 0.05% trypsin (later was inactivated with FBS-containing media). Cell pellets were washed with PBS, centrifuged and resuspended in 200 μL of fresh PBS prior to addition of PI (final concentration of 10 μg/mL) just before fluorescence acquisition. In another set of tubes, trypan blue (final concentration of 0.04%) was used to quench the non-penetrated fluorophore. Fluorescence analysis (at least 10000

events) was performed in a CytoFLEX 15 flow cytometer (Beckman Coulter, Brea, CA, USA) with following diode lasers: 488 nm and 638 nm, 50 mW each. The resulting fluorescence was divided into four channels and detected through band pass filters (Forward scatter area, side scattered area and side scattered width signals) to discriminate the live gates from exclude debris and cell clumps. Dead cells (PI-positive) were omitted with gating in the red channel.

ASSOCIATED CONTENT

Supporting Information

The Supporting Information is available free of charge on the ACS Publication website.

Analytical data (HPLC and HRMS analysis) for peptides **5–13** and **15** and NMR spectra of intermediate organic compounds and **13** and a typical GAMESS input file (PDF).

Molecular formula strings (CSV).

AUTHOR INFORMATIONS

ORCID

Vahid Dianati: **0000-0001-6883-6574**

Pauline Navals: **0000-0002-2703-429X**

Anna Kwiatkowska: **0000-0002-5659-3680**

Yves Dory: **0000-0003-4758-1589**

Robert Day: **0000-0001-8123-1991**

Corresponding Authors

*(RD) Telephone: +1 (819) 821-8000, ext. 75428. E-mail: Robert.Day@USherbrooke.ca and

*(YLD) Telephone: +1 (819) 821 8000 ext. 75299. E-mail: Yves.Dory@USherbrooke.ca

Notes

The authors declare no competing financial interest.

ACKNOWLEDGMENTS

We acknowledge the Canadian Cancer Society Research Institute (701590 to R.D. and Y.L.D.) and Prostate Cancer Canada (TAG2014-02 to R.D.) for their

support. F.C. holds a Banting and Charles Best Canada Graduate Scholarships (grant#315690) from CIHR and Graduate Studentship from Prostate Cancer Canada (Grant #GS-2015-07). We thank Canada Foundation for Innovation, the Ministère de l'Économie et de l'innovation du Québec and the Fonds de recherche du Québec for providing computational facilities and time on the supercomputer mp2 from the Université de Sherbrooke, managed by Calcul Québec and Compute Canada. We also thank Hugo Gagnon and Jean-Philippe Couture (PhenoSwitch Biosciences Inc.) for HRMS analysis.

ABBREVIATIONS USED

PC, proprotein convertase; ADAM, A Disintegrin and metalloproteinase; PCa, prostate cancer; PACE4, paired basic amino acid cleaving enzyme 4; GDF-15, Growth/differentiation factor 15; Amba, 4-amidinobenzylamide; Ampa, 5-(aminomethyl)picolinimidamide; MTT, 3-(4,5-dimethylthiazol-2-yl)-2,5-diphenyltetrazolium bromide; FITC, fluorescein isothiocyanate; DIPEA, *N,N*-diisopropylethylamine; DIAD, diisopropyl azodicarboxylate; NMM, *N*-methylmorpholine; 6-Cl-HOBt, 6-chloro-1-hydroxybenzotriazole; PyBOP,

benzotriazol-1-yl-oxytripyrrolidino-phosphonium hexafluorophosphate; HFIP, hexafluoro-2-propanol DIC, *N*,*N*-diisopropylcarbodiimide; PI, propidium iodide; FBS, fetal bovine serum.

REFERENCES

(1) Klein-Szanto, A. J.; Bassi, D. E., Proprotein convertase inhibition: Paralyzing the cell's master switches. *Biochem. Pharmacol.* **2017**, *140*, 8-15.

(2) Seidah, N. G.; Prat, A., The Biology and Therapeutic Targeting of the Proprotein Convertases. *Nat. Rev. Drug Discov.* **2012**, *11*, 367−383.

(3) Bassi, D. E.; Mahloogi, H.; Klein-Szanto, A. J. P., The Proprotein Convertases Furin and Pace4 Play a Significant Role in Tumor Progression. *Mol. Carcinogen.* **2000**, *28*, 63−69.

(4) Fugère, M.; Day, R., Cutting Back on Pro-Protein Convertases: The Latest Approaches to Pharmacological Inhibition. *Trends Pharmacol. Sci.* **2005**, *26*, 294−301.

(5) Khatib, A.-M.; Siegfried, G.; Chrétien, M.; Metrakos, P.; Seidah, N. G., Proprotein Convertases in Tumor Progression and Malignancy: Novel Targets in Cancer Therapy. *Am. J. Pathol.* **2002,** *160*, 1921−1935.

(6) Couture, F.; D'Anjou, F.; Desjardins, R.; Boudreau, F.; Day, R., Role of Proprotein Convertases in Prostate Cancer Progression. *Neoplasia* **2012**, *14*, 1032−1042.

(7) Longuespée, R.; Couture, F.; Levesque, C.; Kwiatkowska, A.; Desjardins, R.; Gagnon, S.; Vergara, D.; Maffia, M.; Fournier, I.; Salzet, M.; Day, R., Implications of Proprotein Convertases in Ovarian Cancer Cell Proliferation and Tumor Progression: Insights for Pace4 as a Therapeutic Target. *Transl. Oncol.* **2014**, *7*, 410−419.

(8) Panet, F.; Couture, F.; Kwiatkowska, A.; Desjardins, R.; Guérin, B.; Day, R., Pace4 Is an Important Driver of Zr-75-1 Estrogen Receptor-Positive Breast Cancer Proliferation and Tumor Progression. *Eur. J. Cell Biol.* **2017**, *96*, 469−475.

(9) Lin, Y.-E.; Wu, Q.-N.; Lin, X.-D.; Li, G.-Q.; Zhang, Y.-J., Expression of Paired Basic Amino Acid-Cleaving Enzyme 4 (Pace4) Correlated with Prognosis in Non-Small Cell Lung Cancer (Nsclc) Patients. *J. Thorac. Dis.* **2015**, *7*, 850−860.

(10) D'Anjou, F.; Routhier, S.; Perreault, J. P.; Latil, A.; Bonnel, D.; Fournier, I.; Salzet, M.; Day, R., Molecular Validation of Pace4 as a Target in Prostate Cancer. *Transl. Oncol.* **2011**, *4*, 157−172.

(11) Levesque, C.; Couture, F.; Kwiatkowska, A.; Desjardins, R.; Guerin, B.; Neugebauer, W. A.; Day, R., Pace4 Inhibitors and Their Peptidomimetic Analogs Block Prostate Cancer

Tumor Progression through Quiescence Induction, Increased Apoptosis and Impaired Neovascularisation. *Oncotarget* **2015**, *6*, 3680–3693.

(12) Couture, F.; Sabbagh, R.; Kwiatkowska, A.; Desjardins, R.; Guay, S.-P.; Bouchard, L.; Day, R., Pace4 Undergoes an Oncogenic Alternative Splicing Switch in Cancer. *Cancer Res.* **2017**, *77*, 6863–6879.

(13) Levesque, C.; Fugere, M.; Kwiatkowska, A.; Couture, F.; Desjardins, R.; Routhier, S.; Moussette, P.; Prahl, A.; Lammek, B.; Appel, J. R.; Houghten, R. A.; D'Anjou, F.; Dory, Y. L.; Neugebauer, W.; Day, R., The Multi-Leu Peptide Inhibitor Discriminates between Pace4 and Furin and Exhibits Antiproliferative Effects on Prostate Cancer Cells. *J. Med. Chem.* **2012**, *55*, 10501–10511.

(14) Kwiatkowska, A.; Couture, F.; Levesque, C.; Ly, K.; Beauchemin, S.; Desjardins, R.; Neugebauer, W.; Dory, Y. L.; Day, R., Novel Insights into Structure-Activity Relationships of N-Terminally Modified Pace4 Inhibitors. *ChemMedChem* **2016**, *11*, 289–301.

(15) Becker, G. L.; Sielaff, F.; Than, M. E.; Lindberg, I.; Routhier, S.; Day, R.; Lu, Y.; Garten, W.; Steinmetzer, T., Potent Inhibitors of Furin and Furin-Like Proprotein Convertases Containing Decarboxylated P1 Arginine Mimetics. *J. Med. Chem.* **2010**, *53*, 1067–1075.

(16) Dianati, V.; Shamloo, A.; Kwiatkowska, A.; Desjardins, R.; Soldera, A.; Day, R.; Dory, Y. L., Rational Design of a Highly Potent and Selective Peptide Inhibitor of Pace4 by Salt Bridge Interaction with D160 at Position P3. *ChemMedChem* **2017**, *12*, 1169–1172.

(17) Maluch, I.; Levesque, C.; Kwiatkowska, A.; Couture, F.; Ly, K.; Desjardins, R.; Neugebauer, W. A.; Prahl, A.; Day, R., Positional Scanning Identifies the Molecular Determinants of a High Affinity Multi-Leucine Inhibitor for Furin and Pace4. *J. Med. Chem.* **2017**, *60*, 2732–2744.

(18) Henrich, S.; Lindberg, I.; Bode, W.; Than, M. E., Proprotein Convertase Models Based on the Crystal Structures of Furin and Kexin: Explanation of Their Specificity. *J. Mol. Biol.* **2005**, *345*, 211–227.

(19) Huggins, D. J.; Sherman, W.; Tidor, B., Rational Approaches to Improving Selectivity in Drug Design. *J. Med. Chem.* **2012**, *55*, 1424–1444.

(20) Kwiatkowska, A.; Couture, F.; Levesque, C.; Ly, K.; Desjardins, R.; Beauchemin, S.; Prahl, A.; Lammek, B.; Neugebauer, W.; Dory, Y. L.; Day, R., Design, Synthesis, and Structure-Activity Relationship Studies of a Potent Pace4 Inhibitor. *J. Med. Chem.* **2014**, *57*, 98–109.

(21) Lynas, J.; Walker, B., Peptidyl Inverse Esters of P-Methoxybenzoic Acid: A Novel Class of Potent Inactivator of the Serine Proteases. *Biochem. J.* **1997**, *325*, 609−616.

(22) Thompson, R. C., Use of Peptide Aldehydes to Generate Transition-State Analogs of Elastase. *Biochemistry* **1973**, *12*, 47−51.

(23) Dahms, S. O.; Hardes, K.; Becker, G. L.; Steinmetzer, T.; Brandstetter, H.; Than, M. E., X-Ray Structures of Human Furin in Complex with Competitive Inhibitors. *ACS Chem. Biol.* **2014**, *9*, 1113−1118.

(24) MarvinSketch (version 18.1.0 , calculation module developed by ChemAxon, http://www.chemaxon.com/products/marvin/marvinsketch/, 2018.

(25) Ivanova, T.; Hardes, K.; Kallis, S.; Dahms, S. O.; Than, M. E.; Künzel, S.; Böttcher-Friebertshäuser, E.; Lindberg, I.; Jiao, G.-S.; Bartenschlager, R.; Steinmetzer, T., Optimization of Substrate-Analogue Furin Inhibitors. *ChemMedChem* **2017**, *12*, 1953−1968.

(26) Kohn, W.; Becke, A. D.; Parr, R. G. Density Functional Theory of Electronic Structure. *J. Phys. Chem.* **1996**, *100*, 12974-12980.

(27) Couture, F.; Ly, K.; Levesque, C.; Kwiatkowska, A.; Ait-Mohand, S.; Desjardins, R.; Guérin, B.; Day, R., Multi-Leu PACE4 Inhibitor Retention within Cells Is PACE4

Dependent and a Prerequisite for Antiproliferative Activity. *BioMed. Res. Int.* **2015**, *2015*, 1−10.

(28) Tailhades, J.; Gidel, M.-A.; Grossi, B.; Lécaillon, J.; Brunel, L.; Subra, G.; Martinez, J.; Amblard, M., Synthesis of Peptide Alcohols on the Basis of an O-N Acyl-Transfer Reaction. *Angew. Chem. Int. Edit.* **2010**, *49*, 117−120.

(29) Judkins, B. D.; Allen, D. G.; Cook, T. A.; Evans, B.; Sardharwala, T. E., A Versatile Synthesis of Amidines from Nitriles Via Amidoximes. *Synth. Commun.* **1996**, *26*, 4351−4367.

(30) Bondebjerg, J.; Xiang, Z.; Bauzo, R. M.; Haskell-Luevano, C.; Meldal, M., A Solid-Phase Approach to Mouse Melanocortin Receptor Agonists Derived from a Novel Thioether Cyclized Peptidomimetic Scaffold. *J. Am. Chem. Soc.* **2002**, *124*, 11046−11055.

(31) Thomson, D. W.; Commeureuc, A. G. J.; Berlin, S.; Murphy, J. A., Efficient Route to the Pineal Hormone Melatonin by Radical-Based Indole Synthesis. *Synth. Commun.* **2003**, *33*, 3631−3641.

(32) Valdes, H.; Pluháčková, K.; Pitonák, M.; Řezáč, J.; Hobza, P., Benchmark Database on Isolated Small Peptides Containing an Aromatic Side Chain: Comparison between

Wave Function and Density Functional Theory Methods and Empirical Force Field. *Phys. Chem. Chem. Phys.* **2008**, *10*, 2747–2757.

(33) Zhao, Y.; Truhlar, D. G., Density Functionals with Broad Applicability in Chemistry. *Acc. Chem. Res.* **2008**, *41*, 157–167.

(34) Schmidt, M. W.; Baldridge, K. K.; Boatz, J. A.; Elbert, S. T.; Gordon, M. S.; Jensen, J. H.; Koseki, S.; Matsunaga, N.; Nguyen, K. A.; Su, S.; Windus, T. L.; Dupuis, M.; Montgomery, J. A., General Atomic and Molecular Electronic Structure System. *J. Comput. Chem.* **1993**, *14*, 1347–1363.

(35) Molecular Operating Environment (MOE), 2013.08; Chemical Computing Group ULC, 1010 Sherbooke St. West, Suite #910, Montreal, QC, Canada, H3A 2R7, 2018.

(36) Henrich, S.; Cameron, A.; Bourenkov, G. P.; Kiefersauer, R.; Huber, R.; Lindberg, I.; Bode, W.; Than, M. E., The Crystal Structure of the Proprotein Processing Proteinase Furin Explains Its Stringent Specificity. *Nat. Struct. Biol.* **2003**, *10*, 520–526.

(37) Cheng, Y.; Prusoff, W. H., Relationship between the Inhibition Constant (K_i) and the Concentration of Inhibitor Which Causes 50 Percent Inhibition (I_{50}) of an Enzymatic Reaction. *Biochem. Pharmacol.* **1973**, *22*, 3099–3108.

(38) Murphy, D. J., Determination of Accurate Ki Values for Tight-Binding Enzyme Inhibitors: An in Silico Study of Experimental Error and Assay Design. *Anal. Biochem.* **2004**, *327*, 61−67.

(39) Fugere, M.; Limperis, P. C.; Beaulieu-Audy, V.; Gagnon, F.; Lavigne, P.; Klarskov, K.; Leduc, R.; Day, R., Inhibitory Potency and Specificity of Subtilase-Like Pro-Protein Convertase (Spc) Prodomains. *J. Biol. Chem.* **2002**, *277*, 7648−7656.

Table of Content Graphic:

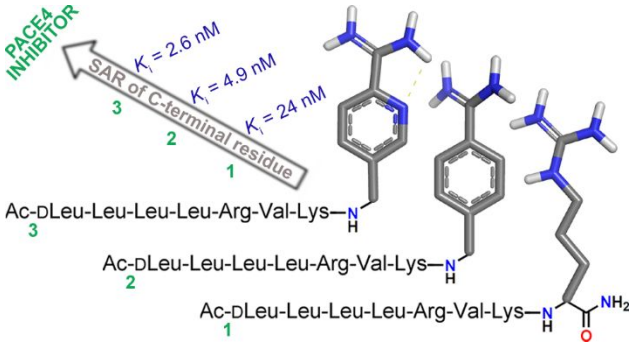

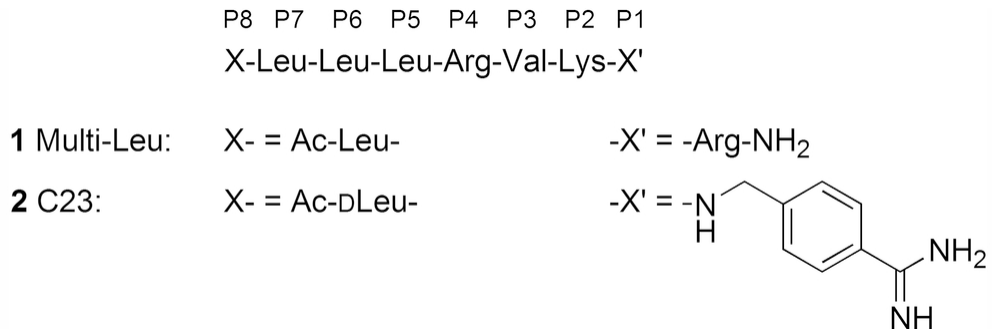

Figure 1. Structure of control PACE4 inhibitors **1** and **2**.

84x27mm (300 x 300 DPI)

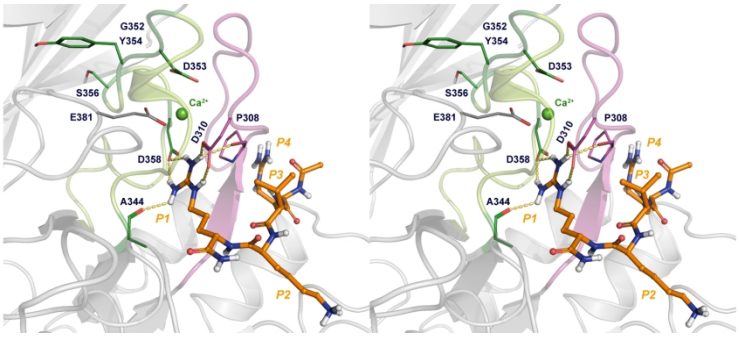

Figure 2. Stereo representation of a PACE4 P1–P4 active site homology model with docked Ac-RVKR-NH_2 (orange) inhibitor. The Ca^{2+} cation (green sphere) located deep inside the S1 subsite is essential for its stability.

177x58mm (300 x 300 DPI)

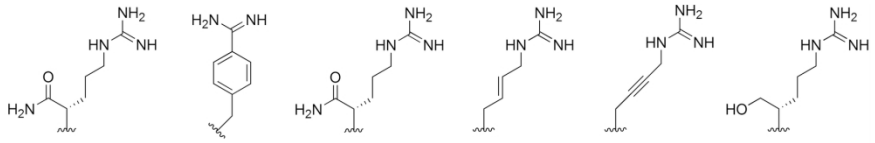

	1[a] Multi-Leu	**2**[b]	**3**[b]	**4**[b]	**5**	**6**
PACE4 K_i (nM):	22 ± 6	4.9 ± 0.9	24 ± 2	13 ± 3	32 ± 4	190 ± 30
Furin K_i (nM):	430 ± 10	9.8 ± 2	760 ± 20	38 ± 4	60 ± 10	250 ± 30
Selectivity:	20	2	32	3	2	9
DU145 IC_{50} (μM):	100 ± 10	25 ± 10	70 ± 30	40 ± 10	110 ± 30	N.C.[c]
LNCaP IC_{50} (μM):	180 ± 10	40 ± 10	150 ± 40	210 ± 20	125 ± 10	N.C.

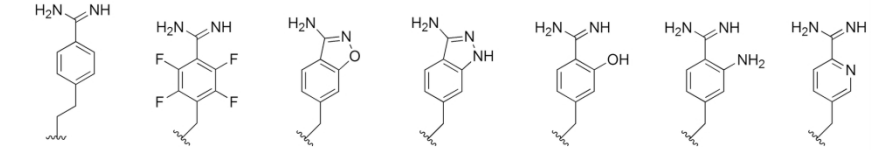

	7	**8**	**9**	**10**	**11**	**12**	**13**
PACE4 K_i (nM):	17 ± 3	240 ± 20	500 ± 130	700 ± 50	53 ± 7	14 ± 4	2.6 ± 0.1
Furin K_i (nM):	41 ± 3	600 ± 100	614 ± 2	825 ± 10	240 ± 20	60 ± 10	21.5 ± 0.9
Selectivity:	2	2	1	1	5	4	8
DU145 IC_{50} (μM):	80 ± 10	69 ± 7	N.D.[d]	N.D.	50 ± 10	61 ± 7	130 ± 20
LNCaP IC_{50} (μM):	80 ± 6	230 ± 50	N.D.	N.D.	113 ± 1	58 ± 7	140 ± 10

Figure 3. Structure of P1 arginine mimetics used for PACE4 inhibitors with general structure of Ac-dLeu-Leu-Leu-Leu-Arg-Val-Lys-NHR apart from **1** [a]with Leu at position P8 instead of dLeu.[13] The inhibition of PACE4 and furin are represented as K_i ± SD, and antiproliferative activity on PCa cell lines as IC_{50} ± SEM. [b]Data adapted from Ref. 14; [c]Not calculable, indicates that the curve did not converged to 50% with doses up to 150 μm; [d]Not determined, due to solubility/precipitation problems.

177x94mm (300 x 300 DPI)

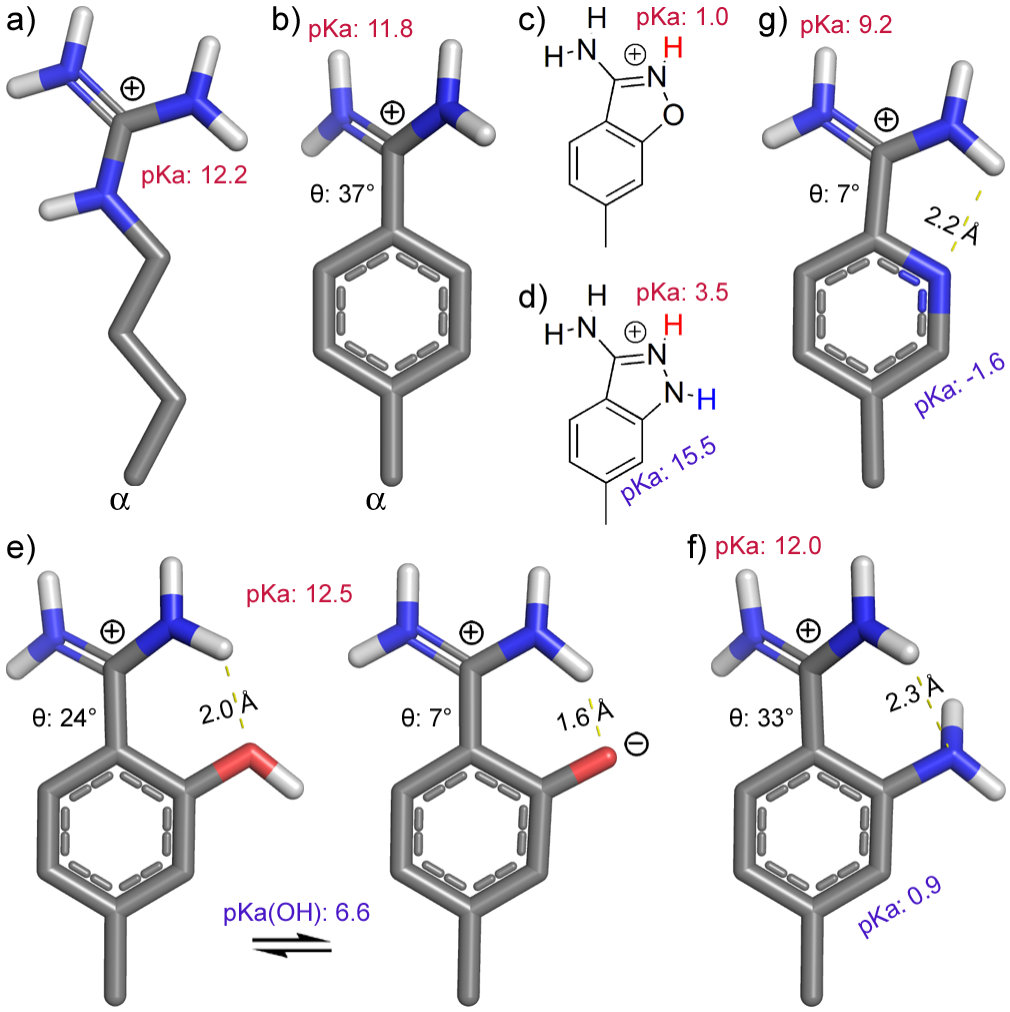

Figure 4. Energy-minimized (DFT) side chain conformers of arginine (**a**) and arginine mimetics (**b**, **e**-**g**) and estimated pKa values of relevant functional groups. Torsion angles between amidine and aromatic planes are shown (θ).

84x84mm (300 x 300 DPI)

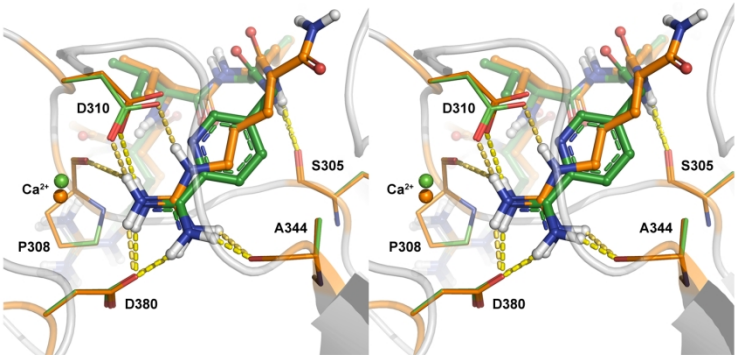

Figure 5. Superimposed *induced fit docking* pose of Ac-RVKX corresponding to the P5-P1 region of compounds **1** (orange) and **13** (green) in the PACE4 homology model active site.[18] Enzyme's side chain C atoms colored the same as corresponding ligand for clarity. H, N and O atoms are in white, blue and red color, respectively. Hydrogen bonds are represented as yellow dashes.

177x62mm (300 x 300 DPI)

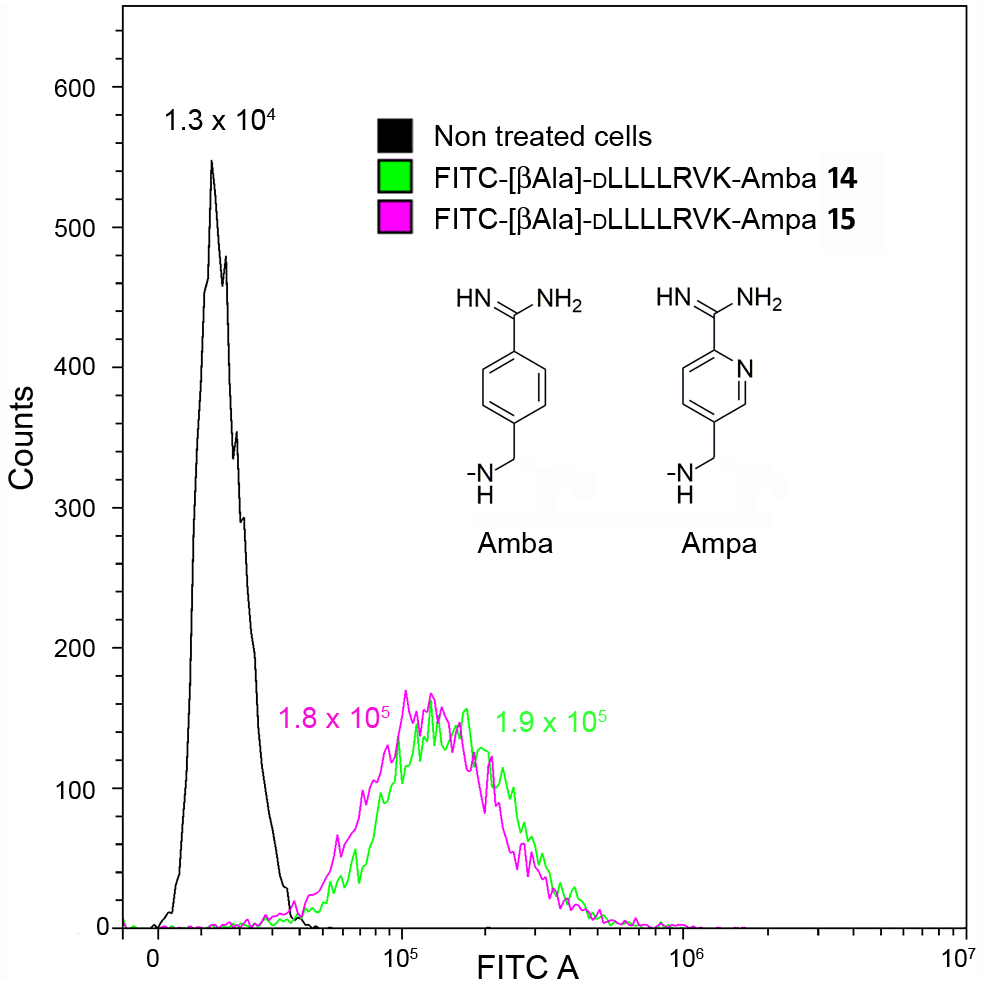

Figure 6. Cell permeability comparison of FITC-labeled analogues **14** and **15** of compounds **2** and **13**.

84x82mm (300 x 300 DPI)

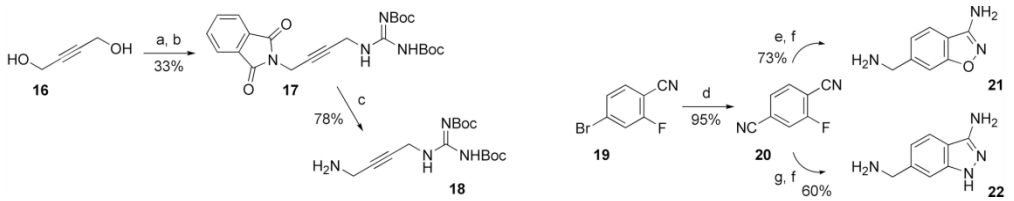

Scheme 1. Synthesis of P1 arginine mimetics 18, 21 and 22 for inhibitors 5, 9 and 10 [a]

[a]Reagents and conditions: (a) phthalimide, DIAD, PPh_3, THF, 0 ^oC to rt, 16 h; (b) N,N'-Di-Boc-guanidine, DIAD, PPh_3, THF, 0 ^oC to rt, 16 h; (c) $N_2H_4.H_2O$, $CHCl_3$/MeOH, 4 h; (d) $Pd(PPh_3)_4$, $Zn(CN)_2$, DMF, 80 ^oC, 6 h; (e) AcNHOH, K_2CO_3, DMF, 12 h; (f) BH_3-THF 1 M in THF, 0 ^oC to rt, 6 h; (g) $N_2H_4.H_2O$, *n*-BuOH, reflux, 16 h.

177x34mm (300 x 300 DPI)

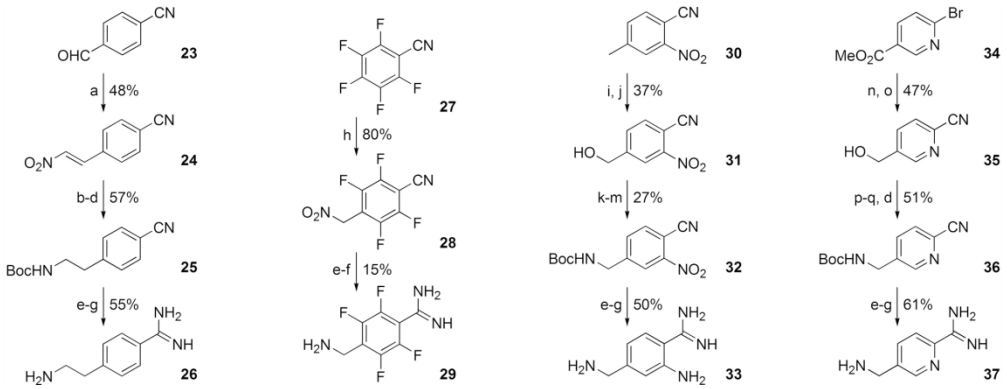

Scheme 2. Synthesis of P1 arginine mimetics 26, 29, 33 and 37 for inhibitors 7, 8, 12 and 13[a]

[a]Reagents and conditions: (a) $MeNO_2$, NaOH, MeOH/H_2O, <10-15 ^oC, 15 min then 5 M HCl; (b) Bu_3SnH, CH_2Cl_2, rt, 16 h; (c) Zn, HCl(aq), 65 ^oC, 1h; (d) $(Boc)_2O$, K_2CO_3, THF/H_2O, 16 h; (e) $NH_2OH.HCl$, DIPEA, MeOH, 60 ^oC, 16 h; (f) Ac_2O, DIPEA, THF then 10% Pd/C, AcOH/MeOH, 35 psi H_2, 12 h; (g) Conc. HCl(aq), MeOH, 0 ^oC to rt, 1 h; (h) $MeNO_2$, TMG, -35 ^oC, 5 min; (i) H_5IO_6, CrO_3, MeCN, 3 h; (j) *i*-BuOCOCl, NMM, THF, 0 ^oC, 2 min then $NaBH_4$ in MeOH, 30 min; (k) TsCl, Et_3N, DMAP, MeCN, 1 h; (l) NaN_3, NaI, DMF, 1 h; (m) PPh_3, H_2O, THF, 16 h then K_2CO_3, $(Boc)_2O$, 16 h; (n) $Pd(PPh_3)_4$, $Zn(CN)_2$, DMF, 100 ^oC, 16 h; (o) $NaBH_4$, LiCl, MeOH, 2 h; (p) phthalimide, DIAD, PPh_3, THF, 0 ^oC to rt, 16 h; (q) $N_2H_4.H_2O$, $CHCl_3$/MeOH, 3 h.

177x67mm (300 x 300 DPI)

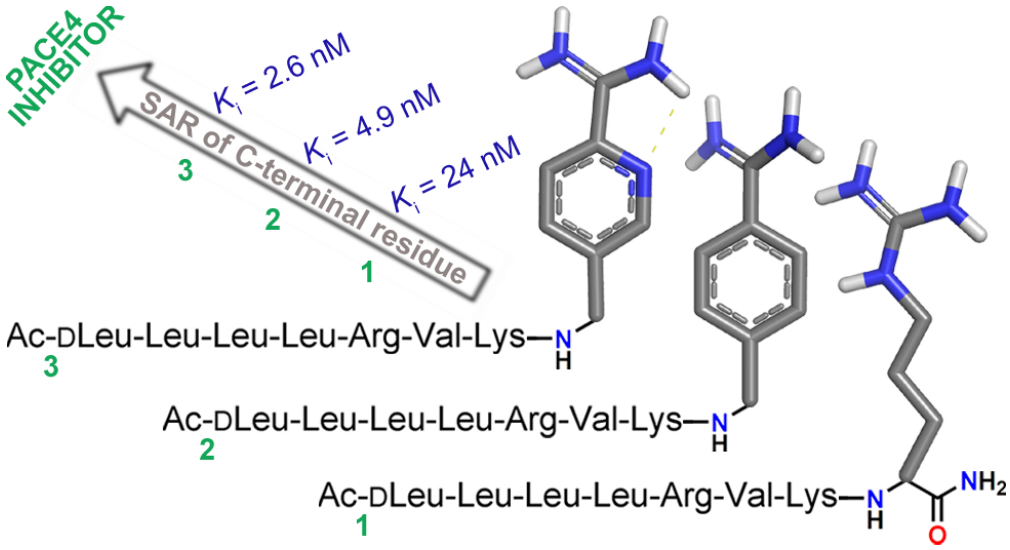

Table of Content Graphic

82x44mm (300 x 300 DPI)